

## Article

# Invasive and Non-Invasive Analyses of Ochre and Iron-Based Pigment Raw Materials: A Methodological Perspective

Laure Dayet

UMR5608 Travaux et Recherches Archéologiques sur les Cultures, les Espaces et les Sociétés,  
Maison de la Recherche, CNRS-Université Toulouse Jean Jaurès, 31058 Toulouse CEDEX 9, France;  
laure.dayet@gmail.com

**Abstract:** Naturally occurring and deeply coloured iron-bearing materials were exploited very early on by human populations. The characterization of these materials has proven useful for addressing several archaeological issues, such as the study of technical behaviors, group mobility, and the reconstruction of cultural dynamics. However, this work poses some critical methodological questions. In this paper, we will review ochre studies by focusing on the analytical methods employed, the limits of non-invasive methods, as well as examples of some quality research addressing specific issues (raw material selection and provenience, heat treatment). We will then present a methodological approach that aims to identify the instrumental limits and the post-depositional alterations that significantly impact the results of the non-invasive analysis of cohesive ochre fragments from Diepkloof rock Shelter, South Africa. We used ochre materials recuperated in both archaeological and geological contexts, and we compared non-invasive surface analyses by XRD, scanning electron microscopy coupled with dispersive X-ray spectrometry (SEM-EDXS), and particle-induced X-ray emission (PIXE) with invasive analysis of powder pellets and sections from the same samples. We conclude that non-invasive SEM-EDXS and PIXE analyses provide non-representative results when the number of measurements is too low and that post-depositional alterations cause significant changes in the mineralogical and major element composition at the surface of archaeological pieces. Such biases, now identified, must be taken into account in future studies in order to propose a rigorous framework for developing archaeological inferences.

**Keywords:** ochre; iron-bearing pigments; characterization; provenance; heat treatment; non-invasive methods; post-depositional alterations



**Citation:** Dayet, L. Invasive and Non-Invasive Analyses of Ochre and Iron-Based Pigment Raw Materials: A Methodological Perspective. *Minerals* **2021**, *11*, 210. <https://doi.org/10.3390/min11020210>

Academic Editor: Domenico Miriello

Received: 1 December 2020

Accepted: 2 February 2021

Published: 17 February 2021

**Publisher's Note:** MDPI stays neutral with regard to jurisdictional claims in published maps and institutional affiliations.



**Copyright:** © 2021 by the author. Licensee MDPI, Basel, Switzerland. This article is an open access article distributed under the terms and conditions of the Creative Commons Attribution (CC BY) license (<https://creativecommons.org/licenses/by/4.0/>).

## 1. Introduction

The earliest uses of coloring minerals date to the Paleolithic during the initial development of *Homo sapiens* on the African continent [1–5]. During these early periods, more than 200,000 years ago, evidence for the use of pigments comes in the form of red and yellow geomaterials, such as rock fragments, that have use-wear traces on their surfaces and were recovered in archaeological deposits. Since these initial periods, deeply coloured iron-bearing rocks were almost continuously used by human populations. They are the primary pigments encountered in rock art, from the Paleolithic to historic periods, and have been used in various contexts, from the decoration of multiple buildings and statues during antiquity and the Middle Ages, to the decoration of the human body, clothes, and traditional artifacts, as has been widely documented in ethnographic reports at a global scale. The success of red to yellow iron-based geomaterials as pigments and for a wide range of other, less documented yet no less important, functions—used for its abrasive or siccative properties, used for protection from UV rays, mosquitoes, or even as a medicinal ingredient, etc. [6–14]—may be related to two characteristics of these minerals. Firstly, iron-bearing deposits are very widespread over the surface of the earth, and secondly, their primary components, iron oxides and oxy-hydroxydes such as goethite, a mineral that produces a brown yellow color, or hematite, whose powder is usually characterized by a

deep red color, have strong staining and coating properties [15]. These are often studied, in both archeology and ethnography, as a single category of material under the broad denomination of “ochre”, although natural hematite and goethite are considered separately in certain contexts [12,16–21]. Much as is done with other mineral resources exploited by humans, their characterization allows for the reconstruction of past technical and symbolic behaviors, of group mobility and social organization, and more generally of cultural dynamics. Broaching these subjects requires bringing to light key information regarding the operational sequences (chaîne opératoire) that bring into play the choices made during raw material acquisition, transformation, and use [2,19,21–33]. The characterization of ochre materials has become an essential part of archeological pigment studies over the last decades, yet such studies are not without their own methodological issues.

Within the fields of archeometry and the archeological sciences more generally, a wide variety of analytical methods and instruments are used to determine both the composition of ochre and its physico-chemical properties. The study of ochre materials from different archeological sites and time periods has revealed that this category is in fact quite heterogeneous, and that it consists in reality of a significant diversity of geomaterials [2,16,17,19,21,24,26,34–39]. They come from various geological formations with different genesis processes and in most cases these formations were submitted to long histories of diagenesis, epigenesis, alteration, and weathering. Thus, ochre materials are composed of various assemblages of minerals and contain an amount of iron oxide or oxyhydroxyde varying from 5–10% to upwards of 90% (in mass oxide). Given the considerable variability that has been documented within this large family of coloring materials, their study requires a dedicated methodology and specific care when broaching their geological origin, provenience, and raw material selection on one hand, and their transformation on the other. Given the heterogeneous nature and irregular shape of ochre materials, both in situ and laboratory analyses may present considerable limits that outweigh the main advantages of non-invasive routine procedures acknowledged in the characterization of industrial materials. In fact, methodological questions arise each time one is confronted with a novel archaeological collection of ochre materials or ochre pigments of any form, despite the many years that these materials have been the focus of dedicated methodological research. In the proceeding sections of this paper, we will review the advantages and disadvantages of the current methods used in ochre characterization as well as the methodological choices that have been made in response to sampling constraints and in function of the archeological question addressed. This discussion will be followed by an evaluation of the accuracy and relevance of non-invasive methods via a comparison of analyses conducted on surfaces of cohesive samples (entire rock pieces whose structure is preserved), powder samples, and polished sections. We will characterize both the instrumental limits and effects of alternations related to post-depositional processes.

## 2. A Broad Methodological Review

### 2.1. *Choosing the Dedicated Methods: An Introduction*

When choosing analytical methods for the characterization of ochre materials, several research parameters must be considered:

- What is the archeological question?
- What is the amount of material, the form of the sample (a piece of rock, residues on a bead, a thin pictorial layer, etc.)?
- Is destructive sampling possible, to which extent?
- Is it a short-term or long-term project?
- What are the facilities I have easy access too?

The two last questions might appear a bit pragmatic, but they are part of the process. They may explain the fact that different choices are made by different authors despite similar research questions and sampling constraints. For this reason, the aim of this review is not to propose a unique methodology but to share some of the most successful solutions that have been developed for ochre characterization in the published literature. Because

of the limited aspect of this paper, we decided to mostly focus on studies of archeological ochre pieces and sediments.

Ochre characterization starts with macroscopic examinations as any other petrologic or mineralogical analyses [21,23,26,30,31,33,40]. The wide range of minerals they are composed of as well as the fine-grained texture they feature as a whole or as a part (their matrix or their cement) constitute limits that are hardly overtaken by simple naked eye or binocular microscope examination [24,28,33,35,37]. In order to take into account their geological and mineralogical diversity, multi-analytical approaches were favoured (Table 1). A common attribute of successful ochre studies is the combination of two main types of analyses: petrographic or mineralogical analyses on one hand; elementary analyses on the other (see e.g., [4,24,25,28,29,32,34,40–47]).

The mineralogical composition of ochre materials can be determined by X-ray diffraction (XRD), Raman spectrometry (RS), Fourier transformed infrared spectrometry (FTIR), petrography, and less frequently by thermogravimetry or Mössbauer spectrometry. X-ray powder diffraction (XRPD) is invasive but it is global, very accurate thanks to exhaustive international reference database such as the PDF (powder diffraction files) from the ICDD (International Centre for Diffraction Data<sup>®</sup>), and also semi-quantitative. Petrography is another destructive method, it requires the preparation of polished thin sections, but its advantage is its high precision in the determination of the arrangement of the minerals and their crystalline nature [16,35,37,42,48,49]. Micro-Raman spectrometry is a point by point method, allowing the analyses of a very small volume, single grains for instance, which makes it ideal for the analyses of ochre powder deposits and coatings, including drawings and paintings [42,50–55]. Scanning electron microscopy coupled with dispersive X-ray spectrometry (SEM-EDXS) allows global elemental analyses but it is also a key method for the identification of mineral phases at the surface of a sample of any form, with or without preparation (residues on artifacts, pictorial layer, cohesive rock, thin section, etc.) thanks to its imagery in back scattered electron highlighting chemical contrasts in combination with X-ray analyses or X-ray cartography (EDXS). If there was one method that could be recommended, this would be the SEM-EDXS. As in any other fields of mineralogy, the combination of several of methods greatly improves the accuracy in the process of identifying mineralogical phases and reduces the risks of confusions between minerals with very broadly similar signals.

In parallel, the whole range of elemental analyses used in geochemistry has been used to characterize ochre materials [17–19,36,38,39,56–65]. The main methods encountered are X-ray fluorescence (XRF, portable or in laboratory), PIXE (particle-induced X-ray emission), inductively coupled plasma and atomic emission spectroscopy (ICP-AES), neutron activation (NAA), or inductively coupled mass spectrometry (ICP-MS, with laser ablation, LA-ICP-MS). They are used to identify major and trace elements in ochre materials. The sensitivity of each instrument is different, NAA and ICP-MS being generally considered as the most sensitive methods for trace element quantification. Detection limits also vary accordingly to the conditions of analyses (see e.g., [39]).

**Table 1.** Non-exhaustive list and short description of studies dedicated to the characterization of archeological ochre materials (mainly cohesive pieces and sediments) during the last two decades.

Reference	Archaeological Issue	Type of Remains	Sampling Limits	Method	Procedure	Sample Preparation
Attard Montalto et al. [60]	Provenance (provenience)	Ochre powders and pieces	None	ICP-AES	Invasive	Grinding, dissolution
Barham [2] (Young [66])	Evidencing human exploitation	Ochre pieces	None	XRD ICP-MS SEM-EDXS	Invasive? Invasive Invasive	? Dissolution Polished blocks
Beck et al. [67]	Classification, provenance (provenience)	Ochre pieces	Use-wear traces on the pieces	PIXE	Non-invasive	None
Belli et al. [68]; Gialanella et al. [43]	Heat treatment	Ochre lumps	None	XRD SEM-EDXS TEM Raman spectrometry	Invasive Invasive Invasive Invasive	Removing of the external part, gentle grinding Same Same, suspension, one drop Same
Bernatchez [69]	Classification	Ochre pieces	None	XRPD PIXE	Invasive Invasive	Grinding, powder Grinding, pellets
Brooks et al. [1]	Evidencing human exploitation, provenance	Ochre pieces	Use-wear traces on the pieces	SEM-EDXS LA-ICP-MS	Non-invasive Minimally invasive	None None
Cavallo et al. [16]	Provenance (provenience)	Ochre pieces	None	Petrography SEM-EDXS	Invasive Invasive	Polished thin-sections Polished thin-sections
Cavallo et al. [70,71]	Provenance (provenience), processing (heat treatment)	Ochre pieces	None	Powder XRD	Invasive	Grinding, powder
Cavallo et al. [32]	Heat treatment	Ochre pieces	None	Powder XRD Petrography SEM-EDXS TEM	Invasive Invasive Invasive Invasive	Grinding, powder Polished thin-sections Polished thin-sections Grinding, suspension, one drop
d'Errico et al. [41]; Salomon et al. [72]	Evidencing human exploitation, heat treatment, provenance (geological origin)	Ochre lumps	Very small collection	SEM-EDXS TEM PIXE-PIGE $\mu$ XRD	Minimally Invasive Minimally Invasive Minimally Invasive Minimally Invasive	Micro-samples, no preparation Micro-samples, suspension, one drop Micro-samples, enrobed in epoxy resin Micro-samples
d'Errico et al. [73]	Raw material classification and selection	Ochre piece	Engraved piece	Visible spectroscopy XRF	Non-invasive Non-invasive	None None
Dayet et al. [28,74]	Raw material classification and selection, heat treatment, provenance (geological origin), changes over time	Ochre pieces	Use-wear traces on the pieces	SEM-EDXS XRD Raman spectroscopy	Non-invasive Non-invasive/invasive Non-invasive	None None/grinding None
Dayet et al. [75]	Raw material classification and selection	Pigment pieces	Use-wear traces on the pieces	SEM-EDXS $\mu$ -XRD Raman spectroscopy pXRF	Non-invasive Non-invasive Non-invasive Non-invasive	None None None None
Dayet et al. [17]	Provenance (provenience), group mobility	Ochre pieces/ferruginous materials	None	XRD ICP-MS ICP-OES	Invasive Invasive Invasive	Grinding, oriented powder Grinding, dissolution Grinding, dissolution

Table 1. Cont.

Reference	Archaeological Issue	Type of Remains	Sampling Limits	Method	Procedure	Sample Preparation
Dayet Bouillot et al. [27]	Raw material classification and selection, heat treatment, provenance (geological origin)	Ochre pieces	Use-wear traces on the pieces	SEM-EDXS XRD Visible spectroscopy	Non-invasive Non-invasive -	None None -
Dayet et al. [29]	Raw material classification, provenance (geological origin), changes over time	Pigment pieces	Museum collection	SEM-EDXS XRD pXRF	Non-invasive Non-invasive Non-invasive	None None None
Domingo et al. [61]	Identification of red pigments, processing and preparation	Pigment pieces and powders	None	SEM-EDXS pXRF XRD FTIR GC (organic part only)	? ? ? ? Likely invasive	? ? ? ? ?
Eiselt et al. [59]	Provenance (provenience)	Ochre pieces and powders	None	NAA	Invasive	Grinding/settling, drying and grinding
Fiore et al. [34]	Technology of paint production	Ochre lumps and sediments	None	XRD FTIR SEM-EDXS GC (organic part only)	? Invasive ? -	? KBr disks ? Crushing, dissolution
Garilli et al. [45]	Provenance (geological origin), heat treatment	Ochre sediments	None	SEM-EDXS XRD ATR-FTIR	Partially invasive Partially invasive Partially invasive	Dried and “homogenized” (method not given) Drying, “homogenized” (method not given) Drying, “homogenized” (method not given)
Godfrey-Smith and Ilani [76]	Heat treatment	Hematite fragments	None	Thermoluminescence XRD	Invasive Invasive	Grinding, extraction of quartz grains Grinding
Goemare et al. [47]	Provenance (geological origin)	Pieces of hematite	Use-wear traces on the pieces	HH-XRF LA-ICP-MS PIXE XRPD	Non-invasive Minimally invasive Non-invasive Invasive	None None None Grinding, extraction of the clay fraction
Goemare et al. [77]	Provenance (geological origin)	Pieces of hematite	Use-wear traces on the pieces	HH-XRF PIXE XRPD Petrography	Non-invasive Non-invasive Invasive Invasive	None None Grinding, extraction of the clay fraction Polished thin-sections
Henshilwood et al. [42]	Evidencing human exploitation, provenance	Lumps and micro-fragments of ochre	None	PIXE SEM-EDXS Petrography $\mu$ XRD	Invasive Non-invasive/invasive Invasive Invasive	Polished thin-sections None/polished thin sections Polished thin-sections Polished thin-sections
Hodgskiss, 2012 [26]	Raw material classification, properties and selection	Ochre pieces	Use-wear traces on the pieces	SEM-EDXS FTIR Raman spectroscopy	Non-invasive Non-invasive Non-invasive	None None None

Table 1. Cont.

Reference	Archaeological Issue	Type of Remains	Sampling Limits	Method	Procedure	Sample Preparation
Hovers et al., 2003 [24]	Provenance (geological origin)	Ochre lumps	None	Petrography XRD ICP-AES	Invasive Invasive? Invasive	Polished thin-sections ? ?
Hughes and Salomon, 2000 [78]	Classification, site comparison	Ochre pieces	None	Dosimetry XRF SEM-EDXS TEM XRD	Invasive ? ? ? Invasive	? ? ? ? Grinding
Lebon et al., 2019 [52]	Raw material selection, links between different human activities	Ochre pieces, powders and residues	None	pXRF SEM-EDXS $\mu$ XRD Powder XRD	Non-invasive Non-invasive Non-invasive Invasive	None None None Grinding
MacDonald et al., 2011 (2013) [18,79]	Site comparison, provenance (geological origin)	Ochre samples	None	NAA	Invasive	Heat-sealed in high-purity polyethylene vials
MacDonald et al., 2018 [19]	Provenance (provenience)	Ochre pieces	Use-wear traces on the pieces	XRD NAA	Non-invasive None-invasive/invasive	None None/grinding
MacDonald et al., 2020 [46]	Raw material properties	Sampling in an ochre mine	None	SEM-EDXS XRD NAA	Invasive Invasive Invasive	? Levigated ?
Matarrese et al., 2011 (Di Prado et al., 2007) [49,80]	Site comparison, provenance (geological origin)	Pigment pieces	None	Petrography XRD	Invasive Invasive	Polished thin-sections Grinding, clay separation
Mathis et al., 2014 [36]	Provenance (geological origin), raw material selection	Ferruginous rocks	None	PIXE	Non-invasive?	None?
Mooney et al. [81]	Provenance (geological origin)	Archaeological ochre	None	Magnetic measurements	Non-invasive	None
Moyo et al. [44]	Raw material characterization, changes over time	Ochre pieces	Samples must not be damaged	XRF XRD FTIR ICP-OES	Non-invasive/invasive Invasive Invasive Invasive	None/grinding Grinding Grinding, KBr pellets Grinding, digestion
Pierce et al. [64]	Provenance (provenience), changes over time	Hematite pieces	None	NAA	Invasive	Grinding
Pradeau et al. [37]	Provenance (provenience), changes over time	Pieces of coloring materials	None/pieces with use-wear traces not analyzed	Petrography SEM-EDXS XRD	Invasive Invasive Invasive	Polished thin-sections Polished thin-sections Grinding
Pomiès et al. [81]	Heat treatment	Ochre pieces	None	XRD TEM	Invasive Invasive	Grinding Grinding, suspension
Popelka-Filcoff et al. [57]	Raw material classification	Ochre lumps and powders	None	NAA	Invasive	Grinding
Roebroeks et al. [4]	Evidencing human exploitation	Ochre sediments	None	XRD SEM-EDXS	Invasive Invasive	Grinding Grinding

Table 1. Cont.

Reference	Archaeological Issue	Type of Remains	Sampling Limits	Method	Procedure	Sample Preparation
Salomon et al. [35] (Salomon [25])	Raw material characterization, heat treatment	Pieces of coloring materials	None/pieces with use-wear traces not analyzed	Petrography SEM-EDXS XRD FTIR TEM	Invasive Invasive Invasive Invasive Invasive	Polished thin-sections Grinding Grinding Grinding Grinding, suspension
Salomon et al. [82]	Heat treatment	Pieces of ferruginous rocks	None	$\mu$ -XRD SEM-FEG TEM-FEG	Non-invasive/minimally invasive Non-invasive/minimally invasive Minimally Invasive	None/micro-samples None/micro-samples Micro-samples?
San Juan-Foucher [83]; Pomiès and Vignaud [84]	Raw material selection, heat treatment	Pieces of coloring materials	None	XRD TEM	Invasive Invasive	Grinding Grinding, suspension
Scadding et al. [62]	Provenance (provenience), raw material selection	Ochre manuports	None	LA-ICP-MS	Minimally invasive	None
Tortosa et al. [48]	Provenance (provenience), changes over time	Ochre fragments	None	XRD ICP-MS Petrography SEM-EDXS XRF	Invasive Invasive Invasive Invasive Invasive	Grinding Grinding Polished thin sections Polished thin sections Grinding
Trabska et al. [65]	Provenance (provenience)	Ferruginous artifacts	None	PIXE XRF	? ?	? ?
Velliky et al. [85] (Velliky et al. [86])	Provenance (geological origin), changes over time	Pigment pieces	None	NAA XRD SEM-EDXS	Invasive Invasive Non-invasive?	? Sub-sampling, grinding None?
Wadley [87]	Taphonomic analysis, accidental heating	Ochre powders	None	XRD XRF ICP-MS Micro-morphology	Invasive Invasive Invasive Invasive	Grinding Grinding Grinding Polished thin sections
Zarzycka et al. [63]	Provenance (provenience), group mobility	Ochre nodules	None	ICP-OES	Invasive	Grinding, dissolution
Zilhao et al. [50]	Evidencing human exploitation	Pigment lumps and residues	None	Powder XRD SEM-EDXS Raman spectroscopy	Invasive Minimally invasive Minimally invasive	Grinding? Micro-sampling Micro-sampling

Choosing between the invasive and non-invasive mode for ochre analysis is more delicate than just choosing a method among a list. As a reminder, by “invasive” we mean that a bit of matter is removed from the object or the sample analyzed, while by “non-invasive” we mean that no matter is removed or destroyed during analysis (totally non-destructive). There are methods that are designed for non-invasive analyses, but they are also often designed for homogenous flat samples, not for heterogeneous and irregular geomaterials. Several methods can be employed in both manners, but the non-invasive mode is often less accurate and/or less sensitive. Each non-invasive technique has its disadvantages in comparison with the equivalent invasive technique. As a consequence, certain archeological issues are still widely addressed by using invasive methods (see Table 1). The main advantages and disadvantages of each non-invasive technique are reviewed here for readers that would not be familiar with their utilization. The methodology developed for the most common archeological issues in ochre studies are described in the following sections.

## 2.2. Non-Invasive Methods Used in Ochre Studies: A Review of Their Limits

Micro-Raman spectroscopy is the most common analytical technique designed for non-invasive analyses. Samples of all sorts and forms, from whole objects to powders, can be placed under a microscope coupled with a Raman spectrometer. The laser beam used in Raman analysis is usually non-destructive for geomaterials. However, oxy-hydroxides such as goethite are very sensitive to the heat induced by the laser, and at high beam power they are turned into hematite [88]. As a consequence, very low laser power is recommended for the analysis of iron oxy-hydroxides in general. Moreover, a spectrum is representative of a very small volume (particle with a diameter of  $<1\ \mu\text{m}$  to  $5\ \mu\text{m}$  with a  $\times 100$  objective, more than  $5\ \mu\text{m}$  for  $\times 50$  objective; [89]), meaning that multiple measurements must be made for large pieces in order to guarantee a representative sampling. Such a necessity may be time consuming for the analysis of a large corpus of pieces, and furthermore makes sample comparison sometimes difficult.

SEM-EDXS, PIXE, micro-XRF, or portable XRF are widely used in non-invasive elemental analyses. The geometry of the samples, however, influences the accuracy of the semi-quantitative (EDXS with classic standards, XRF following the fundamental parameter method) or quantitative (PIXE with dedicated standards; XRF using empirical calibration curves) results. They are more accurate when performed on flat surfaces [90–95]. SEM-EDXS analyses are superficial (the penetration depth is dependent on the atomic number, usually  $<10\ \mu\text{m}$ ) and semi-quantitative. The scanning mode allows for the analysis of areas of several hundred micrometers, but also of small particles of no more than 1 or  $2\ \mu\text{m}$  [96]. This makes SEM-EDXS analyses ideal for the characterization of a matrix or cement that is composed of clay particles with silt and sand-sized inclusions dispersed in it (combination of both semi-quantitative and qualitative approaches; [16,27,37,42,46,74]). Proton beams have a higher penetration depth, but it is still lower than the penetration depth of an X-ray beam [95,97]. PIXE analyses are more sensitive and allow for the quantification of several trace elements, from the transition metals to some rare earth elements. SEM-EDXS and PIXE are designed for the analysis of small surfaces at micrometric scales (not more than  $1\ \text{mm}^2$ ; [98–100]). They can be used for elementary analyses of thin layers because of the low critical penetration depth of secondary X-ray photons produced by primary electron or proton beams [95–97].

The penetration depth of X-ray beams in XRF instruments is dependent on the atomic number of the analyzed material, the anode of the X-ray tube, and the voltage applied [101]. The spatial resolution of XRF analyses, except when using micro-XRF methods, is higher than that of SEM-EDX and PIXE analyses, as the XRF beam is more than 1 mm in diameter and is usually of several millimetres in diameter for portable instruments [98–100]. This higher beam size is advantageous for global analyses of large areas. Nonetheless, a high number of measurements is recommended for the analysis of heterogeneous rocks in order to be assured a high precision [101]. Moreover, matrix effects can be very strong in XRF

analyses, making the quantification of elements complex and time consuming when the samples analyzed have very different mineralogical matrixes (see e.g., [102,103]). The set of trace elements that can be quantified is very variable. XRF can also be carried out at a microscopic scale (micro-XRF), allowing for analyses with a higher spatial resolution, yet the penetration depth of the X-ray beam still remains higher than for other bulk analyses.

In XRD analyses, randomly oriented and oriented powders are the most common preparation modes for heterogeneous inorganic materials. The random mode ensures that the crystals will diffract in random directions and that the diffracted signal collected by the rotating detector will be representative of the proportions of each phase in the sample (no higher intensities due to crystal orientation; [104,105]). Oriented powders are applied on glass plates in order to orient platy particles such as clay minerals. The intensity of clay minerals' main peaks increases, which improves the detection sensitivity and the identification precision of phases from this large mineralogical family [106,107]. Cohesive samples can also be analyzed by classic XRD using Bragg–Brentano geometry. In cases where the crystals are not randomly oriented within the geomaterial, however, XRD peaks whose position do not match that of the rotation circle of the detector will not be detected. The signal collected may therefore not be representative of the overall sample composition. Moreover, if the sample is not flat, angular offsets can be observed between the diffraction signal of the lower and the higher reliefs. This effect can be eliminated by using a parallel beam geometry [74,104]. In micro-XRD, the use of two-dimensional area detectors allows for in situ analyses of minerals within cohesive rocks and polished thin sections, whatever the orientation of the crystals [104]. Micro-XRD analyses are also used for the study of micro-samples in ochre studies [35,72,82].

FTIR analyses were not originally designed for non-invasive characterization. The transmission mode requires the analyst to make KBr pellets in which powder samples are dispersed [108]. A more recent FTIR technique, the attenuated total reflectance (ATR) mode, allows for the analysis of very small amounts of powder or micro-samples. The latter will however be crushed during analysis by the micrometer-controlled compression clamp that is used to make contact between the sample and the crystal, which is a prerequisite to creating an attenuated total reflectance signal [109]. In both cases, the signal collected consists of the vibrational bands of the molecules composing the sample. Non-invasive analyses can only be made in the reflection mode, but the signal obtained is different and more complex. When the reflection mode is used, the vibrational bands of the minerals are not systematically detected. Other parameters than the molecular composition influence the signal in ways that are not predictable (infrared distortion; [110,111]). Only a dedicated referential database, with examples analysed in the same conditions, can allow an accurate interpretation of the spectra and the identification of the minerals present in an unknown sample.

Some invasive methods have been enhanced in order to allow minimally invasive measurements. This is the case with ICP-MS, which can be coupled with a laser ablation system (LA-ICP-MS). The ablation allows for the analysis of very small volume samples, as it forms a small hole with a diameter of some hundreds of micro-meters at the surface of a cohesive sample [1,47,62]. The high spatial resolution of this method can be an advantage or a disadvantage depending on whether a “grain per grain” or global analyses is preferred. In order to counterbalance ochre materials' heterogeneity, some studies propose to carry out multiple measurements per sample [62].

### 2.2.1. Raw Material Characterization of Ochre: Macroscopic Examination versus Physico-Chemical Analyses

Several ochre studies dealing with ochre characterization do not include physico-chemical analyses [21,23,30,33,40,112], or include few physico-chemical analyses with few inferences on raw material characterization [26,113]. Using macroscopic and microscopic examination alone is usually avoided in mineralogical and petrologic studies for several reasons, that could appear trivial when dealing with advanced geological issues: this approach is qualitative; some of the criteria might be subjective; the surface of the rock

might not be representative of the inside (presence of a patina, a layer of alteration); the identification of coarse grains or large crystals within a rock is not always possible; and the fine-grained fraction cannot be properly characterized. Why in this case physico-chemical analyses are not systematically conducted in ochre studies dealing with ochre raw material characterization? There might be a general reason for this choice too, that might appear trivial for archeologists on the other side. Physico-chemical analyses require the access to dedicated facilities and are time consuming. When raw material characterization is not the main goal of the research or might not require a high precision as regard to the research question addressed, macroscopic examination revealed to bring relevant results.

For instance, Watts [23] used several qualitative but strictly defined macroscopic features in order to look for selection criteria amongst raw materials and to question what was the purpose of ochre use for Middle Stone Age people from Pinnacle Point (South Africa). Because he gave very precise definition of each criterion and compares their distribution throughout the sequence independently, his study is reproducible (in theory) and the reliability of the results can be evaluated. Another successful macroscopic study is found in Mauran et al. [33], who inventoried and described various ochre remains (ochre pieces, red deposits on beads, ochre grinding tools, etc.) from the Later Stone Age (LSA) site of Leopard cave (Namibia). Their large but strictly defined categories of ochre raw materials for the characterization of ochre pieces (“iron oxide nodules” versus “various ferruginous rocks”) are just one element among others allowing to discuss the different utilizations of ochre at the site. However, when each raw material category is too accurate to be properly identified from macroscopic criteria (based on silt versus clay texture for instance) and if they are not strictly distinguished one from each other by macroscopic criteria, there is a real risk of inaccuracy. The only way to increase the robustness of the classification is to carry out more accurate mineralogical, petrographic, and elemental analyses. On the other hand, physico-chemical characterization presents a major inconvenience: it requires making a selection of samples. Indeed, the number of pieces within an archeological assemblage is usually high (dozens, hundreds of pieces, sometimes thousands) and certain pieces cannot be destroyed (cultural heritage value). This means that the most accurate analytical methods used in mineralogy and geochemistry cannot be applied to a complete assemblage. Macroscopic examination remains one of the most direct way to characterize a large corpus of archeological ochre pieces.

A final point about ochre raw material characterization concerns the ochre materials themselves. Ferruginous geomaterials present specific features making their characterization complex and difficult in comparison with other families of geomaterials. Iron oxide and oxy-hydroxides commonly form under weathering conditions, which means that there might not be a clear separation of composition between the host rocks and the iron-enriched pedomaterials that are associated to them (see e.g., [15,114,115]). Considering that iron oxides and oxy-hydroxides can also formed within sedimentary rocks, under hydrothermal alteration, in igneous rocks, and can also be found in metamorphic rocks, ferruginous geomaterials are highly diverse and might present heterogeneous petrological features. Their petrological characterization is not trivial. As a consequence, making “raw materials” categories from a collection of ochre pieces is always tricky and there are at least two points that shall be considered in this process according to current research:

- The choice of the geological terms used to name the categories, the best terms probably being those used by geologists in the region of interest (refer to literature on the regional geology; see e.g., [21,26]).
- The fact that intermediate forms between hosts rocks and associated weathering products exist and make absolute classification difficult (see e.g., [17,28]).

### 2.2.2. Ochre Provenance Research

Provenance research allow us to interrogate both the acquisition and circulation of archeological artifacts in various ways. In ochre studies, such approaches tend to be oriented towards: (1) the seriation of archeological pieces in order to discuss their geological

origin; (2) the finding of direct petrological and mineralogical proxies for determining geological origin; (3) the discrimination between geological sources to facilitate future archeological investigations; (4) the comparison of archeological samples with a geological reference collection (provenance or provenience studies *sensu stricto*). The difference between provenance and provenience is discussed elsewhere [39]. We will favour the term “provenience” as proposed by Zipkin et al. [38,39] when referring to issue 4, although the term is not widespread in ochre studies yet. The expression “geological origin” is preferred when sampling allows for only an approximate localization of sources.

Two main approaches have been proposed to investigate ochre provenience and geological origins. In certain cases, petrographic and mineralogical analyses are dominant, while in others, and more frequently moreover, geochemical analyses were favored (Table 2). In the current state of research, these methods are almost all invasive. For example, an in-depth petrological and mineralogical provenance study was carried out by Pradeau et al. [37] on red coloring materials from two Neolithic sites in southeastern France. They used SEM-EDXS analyses on thin sections along with powder XRD analyses in order to identify differences in the rock fabric and the mineralogical composition within a wide range of geomaterials from the region. They were able to distinguish between both local and extra-local sources and used this criterion to discuss the economic patterns observed at the two sites.

**Table 2.** Short description of the various methodologies developed in ochre provenance researches in the last two decades.

Reference	Context	Methods	Mode	Main Goal	Arch. Samples	Geol. Samples	Data Treatment
Barham [2] (Young [66])	Twin Rivers, Zambia	XRF, ICP-MS, SEM-EDXS	Invasive	Seriation, geol. origin	7	-	Qualitative
Hovers et al. [24]	Qafzey, Israël	Pétrography, XRD, ICP-AES	Invasive	Seriation, geol. origin	71	7	Qualitative
Mooney et al. [81]	Australia	Magnetic parameters	Non-invasive	Provenience	2	8	Qualitative
Kiehn et al. [116]	Botswana	NAA	Invasive	Source discrimination	-	72	Multivariate statistical analyses
Popelka-Filcoff et al. [56]	Missouri, USA	NAA	Invasive	Source discrimination	-	69	Multivariate statistical analyses
Popelka-Filcoff et al. [57]	Jiskairumoko, Perou	NAA	Invasive	Seriation	65	-	Multivariate statistical analyses
Trabska et al. [65]	Dzierżysław 35, Poland	PIXE, TXRF	?	Geol. origin	19	11	Multivariate statistical analyses
Bernatchez [69]	Nelson Bay Cave, South Africa	XRD, PIXE	Invasive	Seriation	54	-	Qualitative
Popelka-Filcoff et al. [117]	Arizona, USA	NAA	Invasive	Source discrimination	-	110	Multivariate statistical analyses
Iriarte et al. [118]	Tito Bustillo and Monte Castillo, Spain	Petrography, XRD, SEM-EDS, ICP-MS	Invasive	Source discrimination	-	24 et 24	Qualitative
Salomon [25]; Salomon et al. [35]	Arcy-sur-Cure, France	Macroscopic examination, SEM-EDS, XRD, petrography	Minimally invasive	Seriation, geol. origin	100	-	Qualitative
d’Errico et al. [41]; Salomon et al. [72]	Es Skhul, Israël	XRD, SEM-EDS, PIXE	Minimally invasive	Geol. origin	4	-	Qualitative
Eiselt et al. [59]	Arizona, USA	NAA	Invasive	Provenience	25	54	Multivariate statistical analyses
MacDonald et al. [18]	Canada	NAA	Invasive	Seriation, geol. origin	3	61	Multivariate statistical analyses
Attard Montalto et al. [60]	Malta	Petrography, ICP-AES	Invasive	Provenience	21	58	Multivariate statistical analyses
Beck et al. [67]	Arcy-sur-Cure, France	PIXE	Non-invasive	Seriation, geol. origin	27	-	Qualitative
Popelka-Filcoff et al. [58]	Australia	k0-NAA	Invasive	Source discrimination, comparison between methods	-	100	Multivariate statistical analyses

Table 2. Cont.

Reference	Context	Methods	Mode	Main Goal	Arch. Samples	Geol. Samples	Data Treatment
Kingery-Schwartz et al. [119]	North America, USA	XRD, pXRF, NAA	Non-invasive, invasive	Source discrimination	-	?	Qualitative, multivariate statistical analyses
Mathis et al. [36]	Ormesson, France	PIXE	Non-invasive	Geol. origin	?	29	Bivariate analysis
Zipkin et al. [38]	Northern Malawi	NAA, LA-ICP-MS	Invasive	Source discrimination, comparison between methods	-	22	Multivariate statistical analyses
Dayet et al. [17]	Diepkloof rock shelter, South Africa	XRD, ICP-OES, ICP-MS	Invasive	Geol. origin, provenience	28	80	Qualitative, multivariate statistical analyses
Pradeau et al. [37]	Pendimoun and Giribaldi, France	SEM-EDS, XRD	Invasive	Geol. origin	56	?	Qualitative
Cavallo et al. [16]	Fumane cave and Tagliente Rockshelter Italia	Petrography, SEM-EDXS	Invasive	Geol. origin	?	66	Qualitative
Cavallo et al. [70]	Fumane cave and Tagliente Rockshelter Italia	Powder XRD	Invasive	Geol. origin	?	-	Semi-quantitative
Dimuccio et al. [120]	Grotta della Monica, Italia	pXRF, XRD, Raman, FTIR	Invasive	Source characterization	-	81	Qualitative, multivariate statistical analyses
Zipkin et al. [121]	Central Kenya	LA-ICP-MS	Invasive	Source discrimination	-	43	Multivariate statistical analyses
MacDonald et al. [19]	Haney Cook and Ball villages, Northern America	XRD, NAA	Invasive	Provenience	23	-	Qualitative, multivariate statistical analyses
Velliky et al. [86]	Southwestern Germany	NAA	Invasive	Source discrimination	-	139	Multivariate statistical analyses
Zarzycka et al. [63]	La Prele Mammoth, USA	ICP-OES	Invasive	Provenience	7	24	Multivariate statistical analyses
Peirce et al. [64]	Central Missouri, 4 archaeological sites, USA	NAA	Invasive	Provenience	38	69	Multivariate statistical analyses
Velliky et al. [85]	Hohle Fels, Geißenklösterle and Vogelherd, Germany	NAA, XRD, SEM-EDS	Invasive	Provenience, geol. origin	210	139	Qualitative, multivariate statistical analyses
Zipkin et al. [39]	Central Kenya	LA-ICP-MS	Invasive	Source discrimination	-	36	Multivariate statistical analyses
Mauran et al. [122]	Leopard cave, Namibia	ICP-OES, ICP-MS	Invasive	Geol. origin	41	94	Multivariate statistical analyses

Legend—Geol.: geological; Arch.: archaeological.

The main methods used for investigating major and trace element composition in recent ochre provenance studies were summarized in [39]. Mathis et al. [36] proposed the first complete non-invasive ochre provenance study using a consistent strategy of geological sampling based on strictly defined petrological and contextual criteria (type of rock, geological formation) and PIXE analyses on cohesive unprepared archeological samples. They showed that the iron-rich concretions from the Middle Paleolithic site of Ormesson (France) were collected in a geological formation whose outcrops can be found at no more than 5 km from the site. However, this could represent a particular case given that the number of elements used in the discrimination is low in comparison with the large set of elements used in other provenance studies.

Amongst invasive geochemical approaches, the work from MacDonald et al. [19] is a thorough illustration of how a comprehensive ochre provenance study can be designed. They studied ochre pieces from two Paleoindian sites from the Great Lakes (North America) and compared them to a wide geological collection constituted of samples collected from 10 iron-oxide bearing deposits chosen according to ethnographic, historical, and archeological criteria. They began with petrologic observation and XRD analyses in order to better

characterize the sources. They carried out NAA analyses in order to obtain a large set of trace elements, and they then used multivariate statistical analyses for the discrimination of the elemental signature of the sources. Using the three first principal components of a principal component analysis (PCA) projected on biplots they show that the sources can be graphically discriminated. The projection of archeological samples within these models allow for the identification of their provenience, or at least a geological origin, for the majority of them.

Data treatment is crucial when dealing with the statistical analysis of elemental quantitative results. For ochre studies, there has been some debate on whether elemental data should be log-transformed or not before their use in multivariate analyses [19,38,79,121,122]. It is acknowledged that the use of log-ratios is more suitable when dealing with compositional data [123,124]. Several authors employed log-ratios to iron, following the pioneering work of Popelka-Filcoff and colleagues [56,117]. The main advantages of this data transformation are discussed elsewhere [17,19,39,56,64]. Their interest may however vary according to the choice of the elements that are included in the statistical analysis. There is no consensus on how to select elements in order to allow for the most neutral and efficient discrimination. Looking for the highest degree of discrimination between sources by removing elements following purely statistical procedures when only a limited geological sample is studied might lead to an underestimation of intra-source variability. In such an instance, an archeological sample might not match with a source, despite its geochemical association with it. Putting all elements in the analysis without looking for their relevance in inter-source discrimination might appear to be the most neutral way to avoid such a bias, yet such a practice leads to other biases. In such conditions, the signature of the sources might be very broad and based on very common major or trace elements. An archeological sample might match with such a reference just because it comes from the same geological formation or because it is composed of the same assemblage of minerals.

The method proposed from the beginning by Popelka-Filcoff et al. [56] appears to be a good compromise, as they propose that the most reliable signature of a source is the signature of the iron oxide or oxy-hydroxide phases. They select elements that are positively correlated with iron. Nonetheless, some studies where this method was tested found that no elements were positively correlated with iron when all the sources were included in the process [17,19]. Another limit of this method, which may also explain the first limit discussed, is that iron oxides with high Fe-content are not directly comparable with iron-bearing rocks, as the latter have significantly lower iron contents [17,64]. The use of log-transformed Fe-ratios does not provide a sufficient work-around that smooths the large variations in iron between them. This might be due to geochemical trends that are not entirely understood yet, such as non-linear element migrations, or recrystallization above a threshold of iron concentration, etc. Context-dependent solutions were developed when these limits were encountered [17,19,64].

### 2.2.3. Iron Oxy-Hydroxide Heat Treatment

While ethnographic data suggest that a heat treatment may be part of the operatory sequence of technical gestures preceding ochre use [125], several archeological studies proved this hypothesis to be valuable since Paleolithic times [32,82,126]. The main goal of heat treatment is a change of color. When yellow goethite is heated at a temperature ranging between 260 °C and 300 °C, it turns into red hematite by dehydration:



This is how yellow ochre is converted into red ochre. This well-described reaction is not an oxidation of the goethite phase—the degree of oxidation remains the same—and it is topotactic at a first stage, which means that it does not involve major structural modifications [126–131]. The reaction starts at about 200 °C and is complete at 300 °C. During the process, iron atoms migrate within the octahedral network (position of the oxygen atoms) which results in a “disorder” in the overall structure of the newly formed

hematite. Simultaneously, nano-pores develop inside the crystals where water vapor escapes. When the temperature increases, the structure levels off and pores disappear [43,126]. A recrystallization occurs at temperatures higher than 700 °C.

The main proxies of this transformation are: (1) an anisotropic broadening of hematite X-ray diffraction peaks when the heat temperature is lower than 600 °C; (2) the presence of nano-pores within the precursor goethite crystals observable under SEM-FEG (Field Emission Gun) and TEM (Transmission electron microscopy) techniques [32,43,82,126,130,131] (Table 3). The structural “disorder” of heated goethite is also detected in Raman spectrometry [43,132]. However, the band relating to heating conditions—at about 650–660  $\text{cm}^{-1}$ —is observed in several natural hematites and was interpreted in different ways depending on the authors [132,133]. An anisotropic broadening of X-ray peaks was also detected in some natural hematite samples [126,129]. Whether these samples could have been submitted to incidental heating as in a wildfire for instance has not been investigated yet. Another reaction occurs in goethite if heated in the presence of organic matter. In these very specific conditions maghemite, an iron oxide of an orange-red color ( $\gamma\text{Fe}_2\text{O}_3$ ), is formed [126]. The presence of this iron oxide was also used as a proxy of heating treatment [82,126].

In-depth studies of these different proxies in archeological ochre pieces can be found in, e.g., Gialanella et al. [43], Cavallo et al. [32] and Salomon et al. [82] (see Table 3). The authors of the latter carried out non-invasive and minimally invasive micro-XRD and SEM-FEG analyses along with TEM observations on small micro-samples from several French Upper Paleolithic sites. In particular, they demonstrated that goethite was intentionally heated to produce hematite at the Solutrean site of Les Maîtreaux (France) by showing that the inside and outside of large blocks of hematite show similar patterns of X-ray peak broadening. They estimated the cycle of temperature required to obtain such proxies to be up to 300 to 400 °C for at least two hours. The location of these pieces far from any known combustion feature at the site, in close association with a pile of flint, was further evidence of a heat treatment. Nonetheless, differentiating between intentional and incidental heating is more often a matter of archeological context than a physico-chemical issue (see also [25]).

**Table 3.** Short description of the various methodologies developed for the study of heat treatment features in ochre and iron-bearing geomaterials.

Reference	Context	Arch. Samples	Methods	Experimental Samples	Conditions of Heating Experiments
Onoratini and Perinet [134]	13 Paleolithic sites from south-east France	60	XRPD	11 nat. goethite	
Pomiès et al. [126,129]	5 Paleolithic sites from France	30 + 15	XRPD, TEM	Syn. goethite, 1 nat. goethite	Oven in air 250 to 1000 °C
Baffier et al. [135]	Arcy-sur-Cure, France	3	XRPD, TEM	-	-
Pomiès et al. [136]	Lacaux, France	4	XRPD, TEM	-	-
Godfrey-Smith et Ilani [76]	Qafzeh Cave, Israël	4	TL	-	-
Pomiès and Vignaud [84]; San Juan-Foucher [83]	Bois-Ragot, France	14	XRPD, TEM	-	-
Lahaye [137]	La Honteyre, France	4	TL	-	-
Salomon [25]	Arcy-sur-Cure, France	70	μXRD, TEM	?	?
Salomon [25]; Salomon et al. [82]	Combe-Saunière 1, France	13	μXRD, SEM-FEG, TEM	?	?
Salomon [25]; Salomon et al. [82]	Les Maîtreaux, France	24	μXRD, SEM-FEG, TEM	?	?
Salomon [25]; d'Errico et al. [41]; Salomon et al. [72]	Es-Skhul, Israël	4	μ-XRD, TEM	?	?
Gialanella et al. [43]	Riparo Delmari, Italia	6	XRPD, TEM, Raman	3 nat. goethite	Furnace in air 1000 °C
Salomon et al. [82]	Grotte Blanchard	6	μXRD, SEM-FEG, TEM	?	?
Dayet et al. [27]	Klasies river main site	39	XRD on surfaces	-	-
Cavallo et al. [32]	Fumane cave, Italia	-	XRPD, TEM	-	-
Cavallo et al. [32]	Tagliente rockshelter, Italia	-	XRPD, TEM	-	-

Legend—Arch.: archaeological; Nat.: natural; Syn.: synthetic.

Another method was used more seldomly in case studies for investigating heating features in iron-bearing rocks. Thermoluminescence (TL) techniques are widely known for their capacity to detect the last heating event of a material and to evaluate the age of this event [138]. The same techniques can be applied to determine if an ochre piece was heated if it contains thermoluminescent crystals such as quartz [76,137]. However, again, clear evidence of an intentional heat treatment may not be found.

### 3. Non-Invasive Analyses: A Case Study from Diepkloof Rock Shelter, South Africa

Non-invasive methods, as we showed, present different sorts of limits that have to be considered when choosing them but also when interpreting the results which they provide. This is especially true for archeological artifacts because of a second order of possible biases in non-invasive analyses, that is the preservation of their composition. Their surface in particular might have been submitted to subtle but consistent changes in mineralogical and elemental composition due to various post-depositional phenomenon. In order to address these two methodological aspects, dedicated research can be undertaken.

Here we present a methodological study that was carried out in the framework of a wider research project on the characterization of ochre remains of Diepkloof rock shelter, Western Cape. The main goals of this project were to determine: (1) what kind of raw materials were selected and used; (2) how they were processed; (3) from where and how raw materials were collected; (4) how modalities of ochre exploitation and use vary throughout the sequence. The main constraint we faced was the difficulty of conducting invasive analyses because of the high proportion of ochre pieces showing evidence of use and because of the cultural heritage value of the Middle Stone Age (MSA) collections of Diepkloof rock shelter as a whole. The first steps of the project consisted in performing entirely non-invasive analyses of a large selection of archeological ochre pieces [28,74]. In parallel, when a consistent geological collection of reference was constituted, tests were conducted in order to evaluate the accuracy, the sensitivity, and relevance of the non-invasive protocols used to characterize the archeological samples by comparing them to more conventional bulk and structural invasive analyses. A final step consisted of the selection of a small but representative corpus of 28 archeological ochre pieces for invasive analyses in order to evaluate the influence of post-depositional alterations on the composition of their surfaces, and to evaluate the relevance of previously obtained non-invasive results. These methodological steps are partly described in a PhD thesis [139].

Three methods that can be used in non-invasive and invasive modes were chosen:

- XRD: for structural analyses;
- SEM-EDXS: for bulk analyses of major elements; and
- PIXE: for bulk analyses of major and traces elements.

XRD and SEM-EDS methodological investigations were taken into account in all previously published articles, although they were never properly described [17,27,28]. The PIXE results were never published before.

#### 3.1. Material and Methods

##### 3.1.1. Archeological Samples

Diepkloof rock shelter lies on the west coast of South Africa, about 200 km north of Cape Town. This large quartzitic sandstone shelter overlooking the small Verlorenvlei River valley about 14 km from the present shoreline has been investigated since 1999 by a South African-French team led by J.-P. Rigaud, P.-J. Texier, and C. Poggenpoel. Excavated in three different sectors, the sequence reaches a depth of 3.1 m in the 3 m<sup>2</sup> “main sector” (squares K6, M6, N6) and is mainly composed of MSA deposits [140,141]. The lower stratigraphic units are associated with an estimated date of 110 ky, while the overlying MSA units have been dated to 55 ky by a series of Optically Stimulated Luminescence (OSL) and Thermoluminescence dating [142]. The whole collection of pieces from the main sector (squares M6 and N6) were analyzed in detail [28].

The 27 ochre pieces selected for invasive analyses were either chosen because they had a typical composition among the overall corpus (typical shale, typical ferricrete) or because their composition was intriguing and hard to interpret. Although some pieces with use-wear traces enter in the second category, no piece with clear evidence of use have been destroyed. No other archeological criterion was used to make the selection, although further questions emerged during the provenance research undertaken. Sample selection is always a compromise. Further description of these pieces can be found in [17,28].

### 3.1.2. Geological Samples

The geological samples used in this study come from 12 different sources of raw materials that were collected during several campaigns of survey in a diameter of more than 50 km around Diepkloof rock shelter (Table 4). Five of these sources are shale outcrops (Shale 1 to Shale 5), two are phyllite outcrops that were associated to shale sources (Shale 6 and Shale 7), four are ferricrete from sub-primary deposits (Ferr 1 to Ferr 4), and the last one is associated to a ferricrete deposit (Ferr 2) but it is constituted by indurated shale. Most of these deposits are described elsewhere [17,28]. For the methodological research presented here, 24 samples chosen among all the collected sources were analyzed by XRD (surface, oriented powders) and 5 of them (3 shale/phyllite fragments and 2 ferricrete nodules) were analyzed by EDXS and PIXE (surface, powder pellets).

**Table 4.** Geological outcrops sampled for ochre raw material characterization and provenance studies at Diepkloof rock shelter. Samples from this geological collection were used to investigate the limits of non-invasive application of SEM-EDXS, XRD, and particle-induced X-ray emission (PIXE) analyses on cohesive pieces. Legend—Geol.: geological; Ref.: reference.

Source	Rock Type	Geol. Formation	GPS Coordinates	Nearest Town	Ref.
Shale 1	Shale	Table Mountain	32°23'13" S 18°27'10" E	Elands Bay	14040 to 14055
Shale 2	Shale	Klipheuwel	32°18'57" S 18°21'18" E	Elands Bay	14691
Shale 3	Shale	Klipheuwel	32°27'30" S 18°30'55" E	Redelinghuys	14693
Shale 4	Shale	Klipheuwel	32°29'32" S 18°33'47" E	Redelinghuys	14694
Shale 5	Shale	Table Mountain	32°34'23" S 18°43'50" E	Het Kruis	14692
Shale 6	Phyllite	Malmesbury	32°31'21" S 18°37'56" E	Redelinghuys	14696
Shale 7	Phyllite	Malmesbury	32°52'36" S 18°46'02" E	Piketberg	14700
Ferr 1	Ferricrete	Tertiary/quaternary	32°31'21" S 18°37'56" E	Redelinghuys	14697
Ferr 2	Indurated shale	Tertiary/quaternary	32°42'08" S 18°49'46" E	Eendekuil	14698
Ferr 3	Ferricrete	Tertiary/quaternary	32°42'08" S 18°49'46" E	Eendekuil	14699
Ferr 3	Ferricrete	Tertiary/quaternary	32°52'25" S 18°47'14" E	Piketberg	14701
Ferr 4	Ferricrete	Tertiary/quaternary	32°07'16" S 18°26'30" E	Lamberts Bay	14337

### 3.1.3. Preparation of the Samples

Archeological and geological cohesive pieces were carefully washed by using distilled water and a toothbrush in order to remove all forms of external deposits on them (sediments, soluble salts). For archeological samples, some soluble salts were still detected on the surface of part of the samples despite intense washing. In order to remove the deposits and their superficial part (patina, cortex, any superficial layer which composition might be different from the inside of the piece), the surface of the pieces was abraded against a diamond saw. They were then crushed into powder into an agate mortar. A small quantity of each powder sample was mixed with water and then placed on a glass slide and dried in a 50 °C oven (oriented powder). For EDXS and PIXE analyses, pellets were made. Geological samples were submitted to the exact same protocol.

Before they were ground, a fragment of 7 archeological pieces was extracted by cutting it with a diamond saw. It was enrobed in an acrylic resin under vacuum in order to make polished sections.

### 3.1.4. XRD Analyses

Structural phases were determined by X-ray diffraction. Data were collected with a Bruker D8 Advance diffractometer, equipped with a PSD Linxeye detector and operating with a Cu K $\alpha$  radiation ( $\lambda = 1.5405 \text{ \AA}$ ). Parallel beam geometry (obtained with a Göbel mirror) was used to carry out surface analyses. Bragg–Brentano geometry was used to

analyze oriented powder samples. A 0.3 mm divergent slide was positioned after the X-ray tube with a “knife” placed above the samples in order to cut incident X-rays at low angles and create optimal conditions for detecting clay minerals. The identification of the phases and the semi-quantitative evaluation were done with EVA (Bruker) software (Diffrac.suite). Concentrations calculated in this manner are not truly representative of the proportions of the phases but they are the best proxy we can use to compare the samples. For surface analyses, only the presence/absence of the phases were estimated.

### 3.1.5. SEM-EDXS Analyses

A JEOL 6460 LV SEM (Oxford instruments) instrument was used, equipped with a low vacuum system which allows the imagery and analysis without specific preparation (coating) of the sample. For cohesive samples and powder pellets, we used the *low vacuum* mode with a pressure of 20 Pa and an acceleration voltage of 20 kV. For polished thin sections, a carbon coating was deposited on their surface and EDXS analyses were carried out in *high vacuum*. Semi-quantitative analyses were carried out using EDXS Oxford XMax 20 (Oxford Instruments) spectrometer coupled to the SEM instrument. The spectrometer was calibrated by using the Oxford standards for EDXS analyses. The EDXS results on powder pellets were compared with results of ICP-MS and OES (Optical Emission Spectrometry) analyses of a powder sample from the same ground samples in order to check the accuracy of the EDXS method (Supplementary Materials Table S1).

For pellets and for the surface of cohesive samples, 6 areas were analyzed at  $\times 200$  (surface: about  $300 \mu\text{m}^2$ ). The average and standard deviation were calculated. For the sections, 10 to 13 areas were analyzed along a profile from the edge to the heart of the piece every  $300 \mu\text{m}$ , and at another edge of the piece. The average and standard deviation were also calculated. Three elements were studied in detail: Si, Al, and Fe (major elements in shale and/or ferricrete).

### 3.1.6. PIXE Analyses

PIXE experiments were conducted at the AGLAE (Accélérateur Grand Louvre d’Analyse Élémentaire, Paris, France) facility using a 3 MeV proton extracted beam. The conditions of analyses were chosen according to previous works [67,97]. Because the samples are heterogeneous, they were scanned over a  $500 \mu\text{m}^2$  area. X-ray spectra are recorded by two Si(Li) detectors oriented at  $45^\circ$  to the beam [143]. One is devoted to low energy X-rays (0.1–15 keV) for light elements. The other detector is equipped with selective filters to reduce pileup by attenuating intense X-rays for the detection of heavy elements [144]. We selected the absorber according to the Fe-rich matrix. A  $20 \mu\text{m}$  thick Cr absorber was mounted on the detector. An additional  $50 \mu\text{m}$  thick Al filter was superimposed in order to reduce Cr X-rays induced by the interaction of the primary beam from the sample with the absorber. PIXE spectra were collected between 10 and 15 min in order to obtain more than  $2 \times 10^6$  counts. Because of this long acquisition time, only three analyses per samples were done for the powder and the surface and four for the sections.

Elemental concentrations were extracted by using GUPIX [145]. Parameters were calculated by using a DR-N standard and one of the studied samples (14043a; ICP-MS and ICP-OES measurements used as references). The calculated contents in trace elements V, Ni, Cu, and Zn are significantly different from those measured by ICP-MS (relative difference: more than 20%; Supplementary Materials Table S2). These elements were not taken into account in the present study.

## 3.2. Results

### 3.2.1. XRD Analyses

#### Geological

Our results show that the sensitivity of XRD surface analyses on cohesive samples is lower than the one of XRD on oriented powders (Table 5). For shale and phyllite, anatase and potassic feldspars that present a weak peak on powder X-ray patterns are not detected

on the surface. Clay minerals from the kaolinite and chlorite group are not systematically detected when represented as a minor phase and they are not if the main peak is very weak for powder samples (Figure 1A). This is also true for ferricrete pieces. Quartz and clay minerals from the illite and micas group are well detected in cohesive clay mineral matrixes but not on the surface of ferricrete pieces with a cortex.

**Table 5.** Comparison by XRD between non-invasive analyses on cohesive pieces (surface) and invasive analyses on oriented powders (O. powder) for geological samples. Legend—H: hematite; G: goehite; Q: quartz; I/M: illite/mica; K: kaolinite; Ch: chlorite; P: paragonite; Und. CM: undetermined clay mineral (mixed-layer); PF: potassic feldspar; C: calcite; A: anatase.

Rock Type	Ref.	Mode	H	G	Q	I/M	K	Ch	Pa	Und. CM	PF	C	A
Shale	14042d	O. powder Surface	+ X	- ?	+++ X	++ X	++ X	nd nd	nd nd	nd nd	- nd	- /	- nd
	14043a	O. powder Surface	+ X	- ?	+++ X	++ X	++ X	nd nd	nd nd	nd nd	- nd	- X	- nd
	14045a	O. powder Surface	+ X	- ?	+++ X	++ X	++ X	nd nd	nd nd	nd nd	- nd	- nd	- nd
	14048a	O. powder Surface	++ X	- ?	+++ X	++ X	++ X	nd nd	nd nd	nd nd	- nd	nd nd	- nd
	14050b	O. powder Surface	++ X	? nd	+ /	+++ X	+ X	nd nd	nd nd	nd nd	- nd	nd nd	- nd
	14052a	O. powder Surface	++ X	? nd	+ /	+++ X	+ X	nd nd	nd nd	nd nd	- nd	nd nd	- nd
	14691b	O. powder Surface	+ X	nd nd	+++ X	++ X	+ nd	nd nd	nd nd	nd nd	++ X	- nd	- nd
	14691g	O. powder Surface	+ X	nd nd	+++ X	++ /	+ /	nd nd	nd nd	nd nd	+ /	- nd	- nd
	14691j	O. powder Surface	+ X	nd nd	+++ X	++ X	+ X	nd nd	nd nd	nd nd	+ X	- nd	- nd
	14691k	O. powder Surface	+ X	nd nd	+++ X	++ X	+ nd	nd nd	nd nd	nd nd	+ nd	- nd	- nd
	14693d	O. powder Surface	+ +	nd nd	+++ +++	++ +	- nd	nd nd	nd nd	+ nd	- nd	- nd	nd nd
	14693e	O. powder Surface	+ X	nd nd	+++ X	++ X	- nd	nd nd	nd nd	+ nd	- nd	nd nd	nd nd
	14693g	O. powder Surface	+ -	nd nd	+++ X	++ X	- nd	nd nd	nd nd	+ nd	- nd	nd nd	- nd
	14693j	O. powder Surface	+ X	nd nd	+++ X	++ X	- nd	nd nd	nd nd	+ nd	- nd	- nd	nd nd
	14694e	O. powder Surface	+ X	nd nd	+++ X	++ X	? ?	+ ?	nd nd	nd nd	- nd	nd nd	nd nd
	14692b	O. powder Surface	+ X	nd nd	+++ X	++ X	++ X	nd nd	nd nd	nd nd	nd nd	- nd	nd nd
Phyllite (shale group)	14696c	O. powder Surface	nd nd	nd nd	+ X	+++ X	++ X	nd nd	nd nd	nd nd	- nd	nd nd	nd nd
	14700b	O. powder Surface	nd nd	nd nd	+ X	+++ X	+ X	nd nd	? ?	nd nd	- nd	nd nd	nd nd
Indurated shale (ferricrete group)	14698f	O. powder Surface	+ X	++ X	+++ X	++ X	+ X	nd nd	nd nd	nd nd	+ X	nd nd	nd nd
	14698a (cortex)	O. powder Surface	+++ X	nd nd	? ?	+ nd	++ nd	nd nd	nd nd	nd nd	- nd	nd nd	nd nd
Ferricrete	14697a (cortex)	O. powder Surface	nd nd	+++ X	nd nd	nd nd	nd nd	nd nd	nd nd	nd nd	nd nd	nd nd	nd nd
	14697b (cortex)	O. powder Surface	nd nd	+++ X	+ nd	nd nd							
	14699a (cortex)	O. powder Surface	nd nd	+++ X	- nd	nd nd	+ nd	nd nd	nd nd	nd nd	nd nd	nd nd	nd nd
	14701a (cortex)	O. powder Surface	nd nd	+++ X	++ +	- nd	nd nd						
	14701b (cortex)	O. powder Surface	nd nd	+++ X	nd nd	- nd	nd nd						
	14337a (cortex)	O. powder Surface	+++ X	nd nd	+ nd	nd nd	- nd	nd nd	nd nd	nd nd	nd nd	nd nd	nd nd

Legend—+++ : Main phase; ++: secondary major phases (>10%); +: minor phases (<10%); -: a single small peak; nd: not detected; X: detected, several peaks identified; /: detected, a single peak identified.

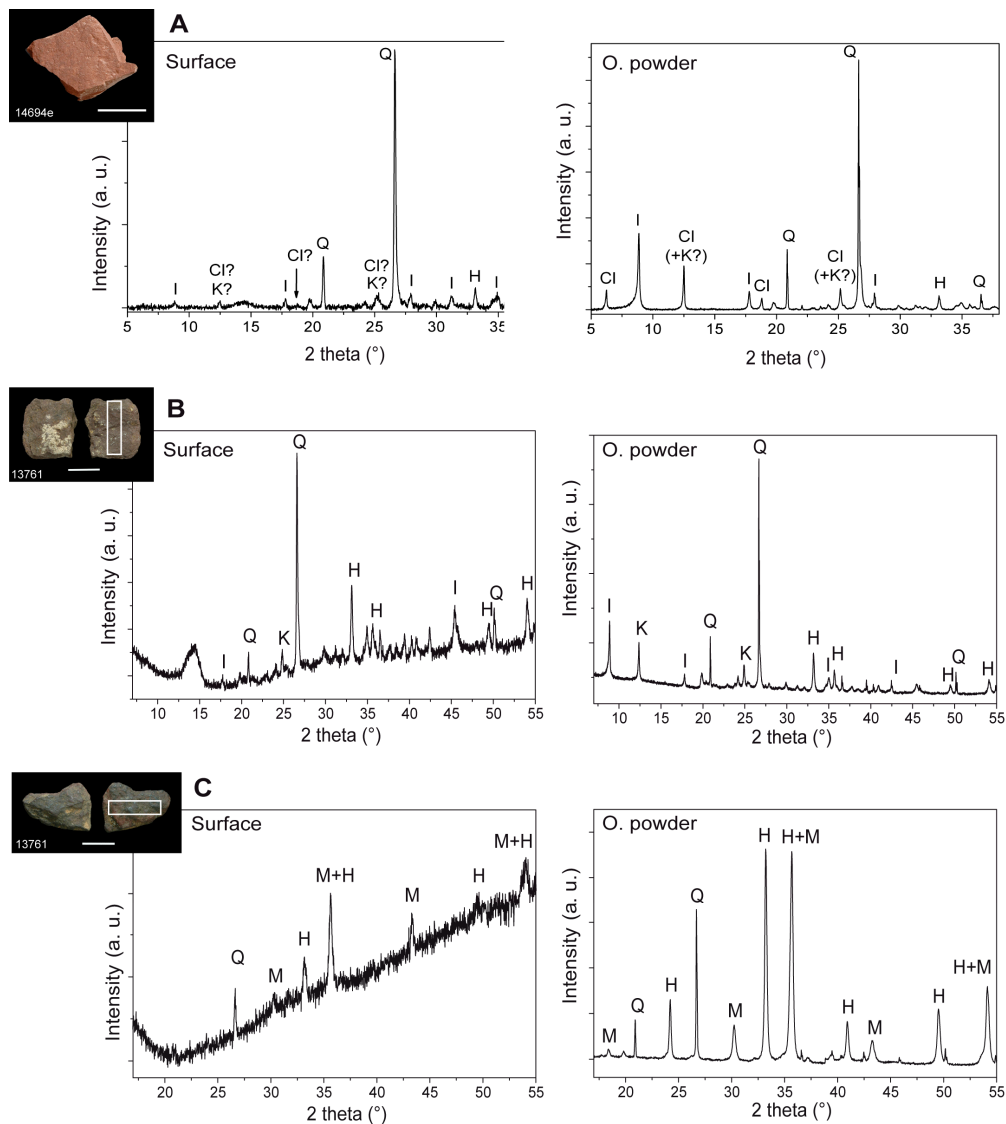


**Figure 1.** XRD patterns of a geological piece of shale (A), an archeological piece of shale (B), and an archeological piece of ferricrete (C): comparison between the surface oriented powder samples (O. powder). Legend—Cl: chlorite; H: hematite; I: illite/mica; K: kaolinite; M: maghemite; Q: quartz; a.u.: arbitrary units.

### Archeological

According to the results described above, phases with a single weak peak on the powder X-ray patterns (mainly anatase, potassic feldspar, calcite) were not used to compare archeological samples. When doing so, more than half of the archeological pieces show identical results for phase detection whatever analyzed on the surface or as powder samples. Quartz and kaolinite are more systematically found in powder samples than in cohesive samples for both shale and ferricrete pieces (Table 6; Figure 1B,C). Clay minerals whatever their type are never detected in ferricrete or intermediate raw materials (ferr/shale), especially those exhibiting a cortex (Figure 1C). Interestingly, archeological ferricrete samples which do not show a highly developed cortex do not contain clay minerals at all (below the detection limit of powder oriented XRD analyses).

In certain shale and ferricrete pieces, maghemite is detected on the surface of the samples but not in the powder. Hematite is not detected on the surface of two samples despite it is present in the powder; the main iron oxide observed in both the surface and

the powder is maghemite (13716; 13777). Goethite is not detected on the surface of another sample despite being detected in the powder, hematite being identified instead (13722).

**Table 6.** Comparison between non-invasive analyses on cohesive pieces and invasive analyses on oriented powders by XRD for archeological samples. Legend—\*: proxy for geological origin; in bold: main phase detected.

Rock Type	Ref.	Oriented Powder	Surface	Difference of Composition
Shale/sandstone	13716	Quartz, I/M, maghemite, hematite	Quartz, maghemite	Heat, sensitivity
Shale	13681	Quartz, I/M, kaolinite, hematite	Identical	-
Shale	13711	I/M, quartz, hematite, kaolinite	Identical	-
Shale	13715	Quartz, I/M, kaolinite, hematite	Identical	-
Phyllite	13718	I/M, hematite	Identical	-
Shale	13723	Hematite, I/M, pyrophyllite *	Identical *	-
Shale	13752	I/M, quartz, hematite, goethite, kaolinite, anatase	Quartz, I/M, hematite, goethite	Sensitivity
Shale	13757	I/M, kaolinite, quartz, hematite, anatase	Kaolinite, I/M, hematite	Sensitivity, patina?
Shale	13758	Quartz, kaolinite, I/M, hematite	Identical	-
Shale	13761	I/M, quartz, hematite, kaolinite	Identical	-
Shale	13771	I/M, quartz, hematite	I/M, hematite	Patina?
Shale	13773	Quartz, hematite, I/M, kaolinite	Identical	-
Shale	13777	Quartz, kaolinite, I/M, hematite	I/M, maghemite	Heat, sensitivity, patina?
Shale	13783	I/M, quartz, hematite, kaolinite	Identical	-
Shale	13804	Quartz, I/M, hematite, kaolinite	Identical	-
Ferr/shale	13725	Hematite	Hematite, quartz (maghemite?)	Cortex
Ferr/shale	13727	Maghemite, hematite, quartz	Identical	-
Ferr/shale	13750	Hematite, I/M, kaolinite	Hematite, quartz	Sensitivity, cortex
Ferricrete	13712	Hematite	Identical	-
Ferricrete	13690	Maghemite, hematite, quartz	Identical	-
Ferricrete	13722	Goethite, kaolinite, hematite, quartz	Hematite	Heat, sensitivity, cortex
Ferricrete	13724	Hematite, quartz	Maghemite, hematite, quartz	Heat
Ferricrete	13741	Hematite, quartz	Identical	-
Ferricrete	13743	Hematite, maghemite	Hematite	Heat
Ferricrete	13749	Hematite, maghemite	Identical	-
Ferricrete	13762	Hematite, quartz, kaolinite	Quartz, hematite	Sensitivity, cortex
Ferricrete	13793	Hematite, maghemite, quartz	Maghemite, hematite	Cortex

### 3.2.2. SEM-EDXS Analyses Geological

When powder and cohesive geological samples are compared, we observe a relatively good adequacy for four samples (three shale and one ferricrete), and great discrepancy for one ferricrete in Si, Al, and Fe contents (Table 7; Figure 2). The latter is composed of a crypto-microcrystalline matrix of iron oxide in which coarse quartz grains are heterogeneously dispersed. The area of analysis is too small to overcome this great textural heterogeneity. The texture of the other samples is more homogenous under the scale of analysis chosen (Figure 3). The relative difference between the two averages (surface and powder) is lower than 10% for three of them and lower than 20% for the last one. This difference remains acceptable and could probably be improved by increasing the number of analyses for cohesive samples.

**Table 7.** Comparison by EDXS between non-invasive analyses on cohesive pieces (surface) and invasive analyses on powder pellets (powder) for geological samples. Results were normalized to 100% by using a conventional list of elements (ICP-OES data). Legend—SD: standard deviation.

Sample	Mode	Measurement	Na <sub>2</sub> O	MgO	Al <sub>2</sub> O <sub>3</sub>	SiO <sub>2</sub>	P <sub>2</sub> O <sub>5</sub>	K <sub>2</sub> O	CaO	TiO <sub>2</sub>	MnO	Fe <sub>2</sub> O <sub>3</sub>	Total
14043a	Surface	AVERAGE	0.5	0.7	24.2	56.5	0.7	5.1	nd	1.2	nd	11.0	100.0
		SD	0.0	0.1	0.5	1.2	0.1	0.2	-	0.1	-	1.1	-
	Powder	AVERAGE	0.5	0.9	25.0	55.9	0.4	5.0	0.1	1.1	0.1	11.0	100.0
		SD	0.1	0.0	0.2	0.6	0.1	0.0	0.0	0.1	0.1	0.3	-
14050b	Surface	AVERAGE	0.3	1.0	25.2	47.9	0.7	6.4	0.1	1.4	0.1	16.9	100.0
		SD	0.0	0.1	0.9	1.3	0.2	0.3	0.1	0.2	0.1	1.5	-
	Powder	AVERAGE	0.8	1.2	26.2	46.5	0.5	6.3	0.3	1.3	0.1	16.7	100.0
		SD	0.0	0.0	0.1	0.1	0.1	0.0	0.0	0.1	0.0	0.1	-
14696c	Surface	AVERAGE	7.2	2.5	24.0	52.4	nd	4.8	nd	1.1	nd	8.0	100.0
		SD	0.8	0.1	1.9	1.0	-	0.4	-	0.1	-	0.4	-
	Powder	AVERAGE	2.4	2.1	27.0	55.8	nd	5.7	0.1	1.0	nd	6.0	100.0
		SD	0.3	0.2	0.3	0.3	-	0.1	0.1	0.1	-	0.2	-

Table 7. Cont.

Sample	Mode	Measurement	Na <sub>2</sub> O	MgO	Al <sub>2</sub> O <sub>3</sub>	SiO <sub>2</sub>	P <sub>2</sub> O <sub>5</sub>	K <sub>2</sub> O	CaO	TiO <sub>2</sub>	MnO	Fe <sub>2</sub> O <sub>3</sub>	Total
14697a	Surface	AVERAGE	1.4	0.4	3.9	2.9	1.9	0.1	0.1	0.1	nd	89.3	100.0
		SD	1.3	0.1	1.1	0.6	0.2	0.1	0.1	0.2	-	3.3	-
	Powder	AVERAGE	0.4	0.5	4.0	2.5	2.5	0.1	0.2	nd	nd	89.7	100.0
		SD	0.0	0.1	0.4	0.1	0.1	0.0	0.0	-	-	0.4	-
14699a	Surface	AVERAGE	0.1	0.1	8.2	6.3	3.9	0.2	0.1	nd	nd	81.0	100.0
		SD	0.1	0.1	5.3	8.0	1.0	0.2	0.1	-	-	12.7	-
	Powder	AVERAGE	0.2	0.2	17.7	17.7	3.3	0.4	nd	0.1	nd	60.4	100.0
		SD	0.0	0.0	0.2	0.2	0.1	0.0	-	0.1	-	0.4	-

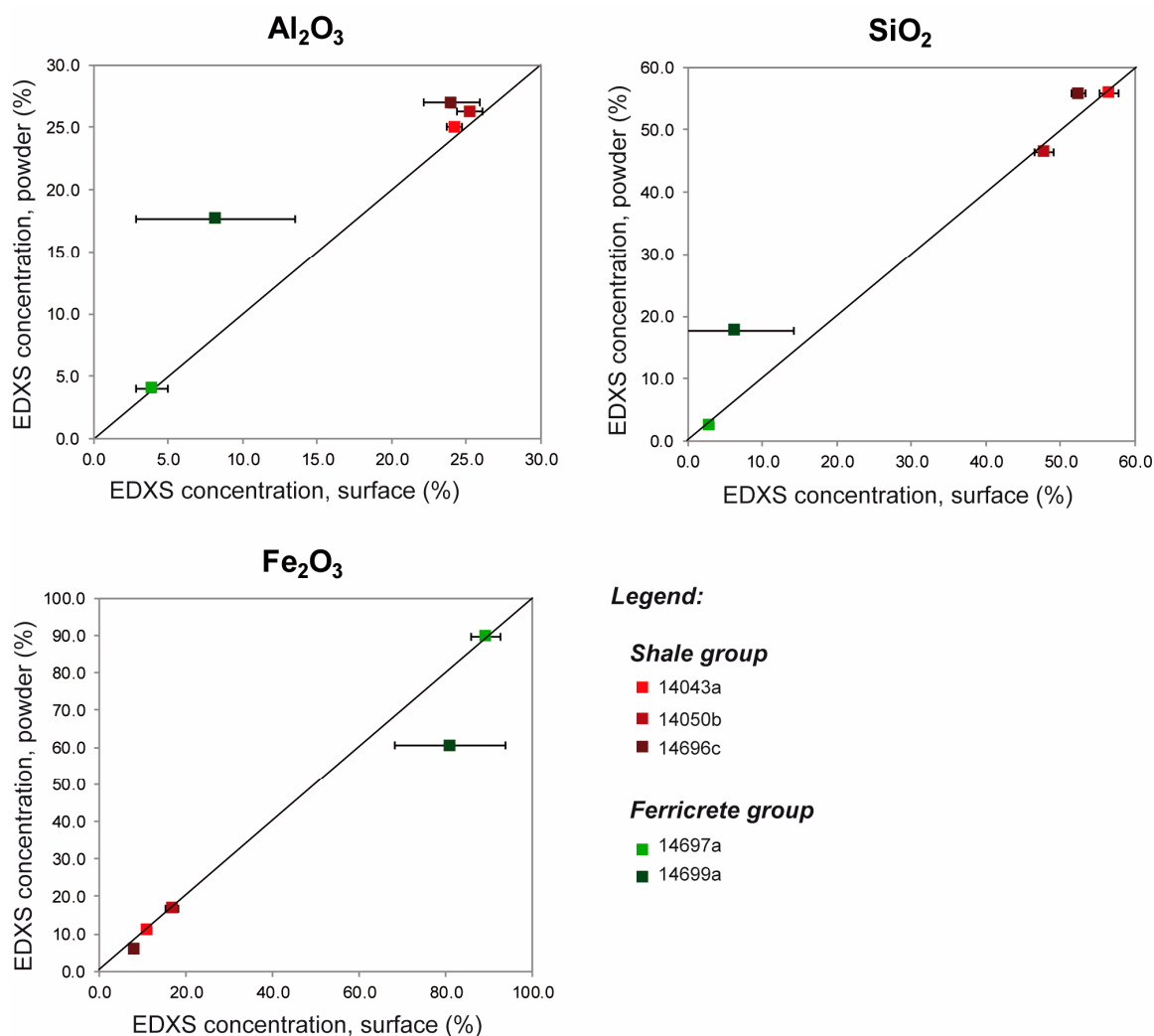
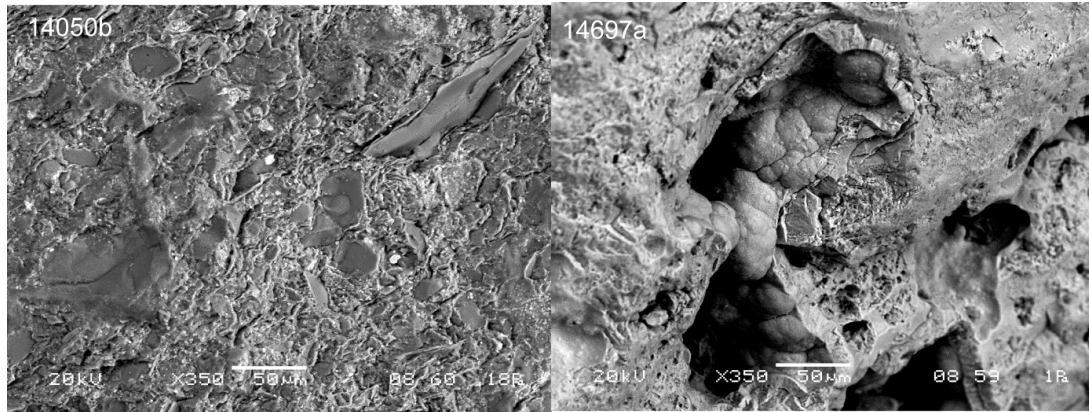


Figure 2. Results of EDXS analyses of cohesive geological pieces (surface) compared with the analysis of pellets (powder) for major elements Al, Si, and Fe.

Archeological

The comparison between the measurements on the surface and the section shows that small quantities of soluble salts remain at the surface. Elements Na, Mg, P, and Ca are in higher concentration at the surface relative to the section of the ferricrete and shale pieces (<1.5% in mass oxide; Figure 4; Supplementary Materials Table S3). They form a surficial layer of water soluble minerals. The concentration in Si is significantly lower on the surface of three samples, the two shale pieces (13681 and 13773) and one ferricrete piece (13690) (Figure 4). The absolute difference is of 9% to 16%. In two ferricrete pieces, Fe content is a bit lower on the surface (13712, 13741) while it is a bit higher in one shale piece (13681), and Al content is higher in the other shale piece (13773). The high decrease in Si

content at the surface of the samples can be interpreted as the presence of a thin coating of quartz grains. In ferricrete pieces, the formation of a patina or a cortex might lead to slight Fe impoverishment.



**Figure 3.** SEM images (BSE, back scattered electron mode) of the surface of two geological pieces studied, showing the coarse inclusions in one shale (14050b) and the matrix of iron oxide crystals in one ferricrete (14697a).

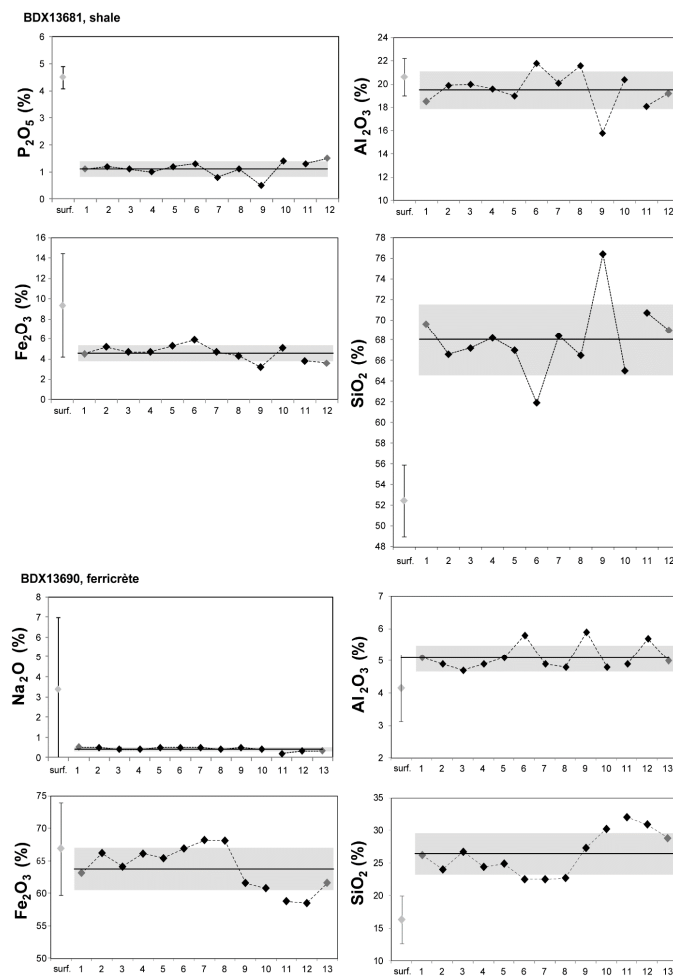


**Figure 4.** Main EDXS results of two archeological pieces, a shale (13681) and a ferricrete (13690): comparison between the surface and the section. Diamonds in light gray: average with standard deviation calculated from six measures on the surface. Diamonds in dark gray: edges of the section. Diamonds in black: inside of the section. The black line represents the average from the measurements on the section and the gray area the standard deviation. Legend—Surf.: Surface.

3.2.3. PIXE  
Geological

The adequacy between powder and surface analyses for geological samples is lower for PIXE analyses than for EDXS analyses. It is mostly Al and Si contents that are affected (Figure 5; Table 8). The surface of a shale sample (14696c) is noticeably enriched in Na and Cl, explaining the discrepancies observed. For the rest of the samples, the absence of compositional pattern suggests that the number of analyses carried out at the surface was too low to overcome heterogeneity problems. With regard to trace elements, a good adequacy between the surface and pellets is observed for Ga, As, Rb, Y, Nb, Pb, and Th: the  $R^2$  is systematically higher than 0.95 (Figure 5).

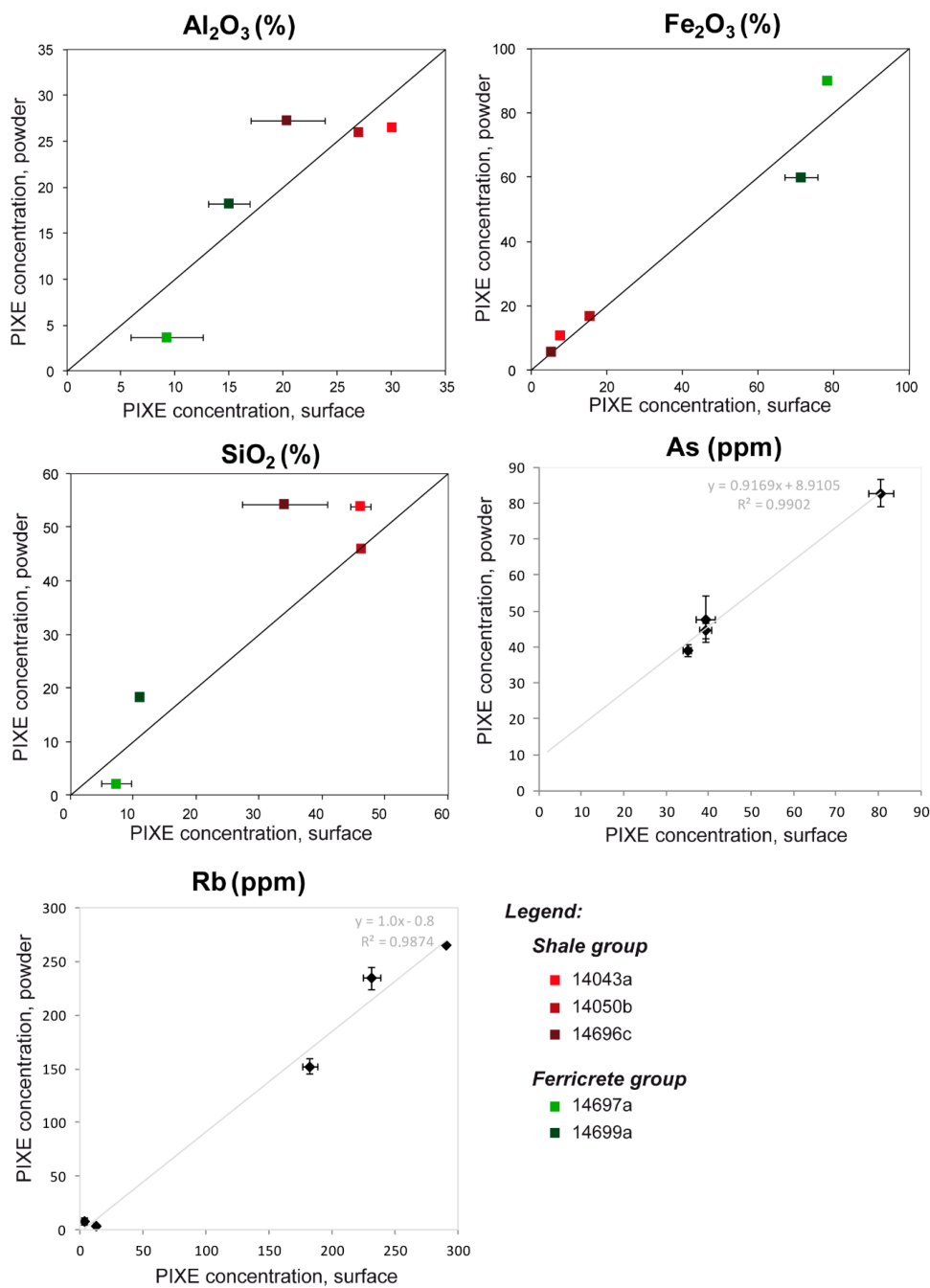


Figure 5. Results of PIXE analyses of cohesive geological pieces (surface) compared with the analysis of pellets (powder) for major elements Al, Si, and Fe, as well as trace elements Rb and As.

**Table 8.** Comparison by PIXE between non-invasive analyses on cohesive pieces (surface) and invasive analyses on powder pellets (powder) for geological samples. Results were normalized to 100% by using all elements quantified by PIXE. Legend—nd: not detected.

Sample	Mode	Measurement	Na <sub>2</sub> O %	MgO %	Al <sub>2</sub> O <sub>3</sub> %	SiO <sub>2</sub> %	P <sub>2</sub> O <sub>5</sub> %	SO <sub>3</sub> %	Cl %	K <sub>2</sub> O %	CaO %	TiO <sub>2</sub> %	MnO %	Fe <sub>2</sub> O <sub>3</sub> %	Cr ppm	Ga ppm	As ppm	Rb ppm	Sr ppm	Y ppm	Zr ppm	Nb ppm	Ba ppm	Pb ppm	Th ppm
14043a	Surface	AVERAGE	1.6	0.5	30.1	46.0	4.5	1.3	2.4	4.0	0.2	1.0	0.05	7.7	64	26	48	152	290	48	394	22	443	58	23
		SD	0.3	0.0	0.3	1.6	0.6	0.1	0.1	0.1	0.0	0.2	0.00	1.1	5	4	6	26	39	7	28	8	215	13	3
	Powder	AVERAGE	0.4	0.7	26.5	53.9	0.3	0.1	0.3	4.9	0.1	1.4	0.06	10.4	71	32	39	183	147	50	439	25	660	50	22
		SD	0.0	0.0	0.2	0.2	0.0	0.0	0.1	0.0	0.0	0.01	0.4	19	2	2	3	7	6	107	3	155	4	2	
14050b	Surface	AVERAGE	0.2	0.8	27.0	46.2	0.4	0.9	0.1	6.1	0.1	1.8	0.09	15.5	155	38	83	234	204	76	351	33	669	68	32
		SD	0.0	0.0	0.3	0.5	0.0	0.3	0.0	0.2	0.0	0.1	0.01	0.2	6	0	4	9	13	11	36	3	106	2	2
	Powder	AVERAGE	0.5	0.9	26.0	46.0	0.3	0.3	0.5	6.0	0.3	1.7	0.09	16.5	130	37	81	232	201	74	334	34	608	67	27
		SD	0.1	0.0	0.1	0.3	0.0	0.1	0.0	0.0	0.0	0.00	0.2	32	2	3	3	3	7	75	4	246	5	4	
14696c	Surface	AVERAGE	13.5	2.4	20.3	33.8	0.2	3.2	18.1	4.1	0.1	1.0	nd	4.7	67	24	nd	265	75	31	327	19	592	9	30
		SD	6.7	0.5	3.4	6.7	0.0	6.2	0.5	0.0	0.2	-	0.2	33	1	-	15	9	1	301	4	118	3	7	
	Powder	AVERAGE	1.9	1.5	27.3	54.3	0.0	0.2	3.1	5.3	0.1	1.0	0.01	4.8	109	27	2	291	70	37	204	17	599	9	25
		SD	0.1	0.1	0.2	0.1	0.0	0.1	0.2	0.0	0.0	0.00	0.2	53	1	-	-	7	13	60	2	174	1	6	
14697a	Surface	AVERAGE	0.8	0.5	9.2	7.2	1.6	0.7	0.4	0.3	0.1	0.1	nd	78.3	nd	5	39	8	378	4	23	2	3068	12	11
		SD	0.1	0.1	1.9	2.2	0.2	0.1	0.1	0.1	0.0	0.0	-	4.3	-	1	2	3	8	3	6	0	456	1	4
	Powder	AVERAGE	0.3	0.3	3.7	2.2	1.8	0.5	0.5	0.1	0.2	nd	nd	90.1	59	5	35	4	55	5	18	3	441	nd	8
		SD	0.0	0.0	0.1	0.1	0.0	0.0	0.0	0.0	0.0	-	-	0.6	37	-	1	2	4	2	1	1	140	-	1
14699a	Surface	AVERAGE	0.2	0.3	15.0	11.0	1.4	0.2	0.0	0.2	0.1	0.2	nd	71.4	117	15	45	4	13	9	32	2	86	30	6
		SD	0.0	0.0	0.1	0.4	0.0	0.0	0.0	0.0	0.0	0.0	-	0.4	47	1	2	1	1	1	3	6	40	1	-
	Powder	AVERAGE	0.1	0.2	18.2	18.3	2.4	0.1	0.0	0.4	0.0	0.1	nd	59.9	98	5	39	13	8	6	16	2	79	25	nd
		SD	0.0	0.0	0.2	0.3	0.1	0.0	0.0	0.0	0.0	-	-	0.5	31	1	2	2	2	2	4	-	-	4	-

Archeological

The analyses of five sections confirms that the surface of the pieces is enriched in Na, Mg, P, and Ca (Supplementary Materials Table S4). In addition, Si concentrations are significantly much lower in all shale or shale/sandstone pieces (13681; 13715; 13716; 13773; Figure 6A) and it shows variations in the inside of the ferricrete (13741). Al contents are a bit higher in two shale pieces (13681; 13773). This is consistent with the main tendency observed by EDXS and allows to refine some of the hypotheses proposed above: quartz grains might be covered by a thin coating, sometimes enriched in Al; coarse quartz grains are heterogeneously distributed in certain ferricrete pieces.

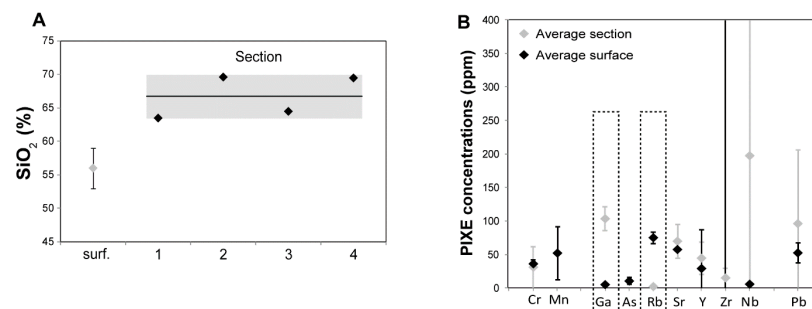


**Figure 6.** Main PIXE results for a piece of shale/sandstone (13716): comparison between the surface and the section. (A) Results for the major element Si. Diamonds in light gray: average with standard deviation calculated from three measures on the surface. Diamonds in black: inside of the section. The black line represents the average from the measurements on the section and the gray area the standard deviation. (B) Results for trace elements (average and standard deviation only). Legend—Surf.: Surface.

Tendencies in trace element contents are very variable depending on the trace element and the raw material considered. For shale pieces, the distribution of Zr and Ba is heterogeneous (high standard deviation; Figure 6B). This may explain the low adequacy between powder and surface in geological samples. The adequacy between the surface and the section is quite good in all samples for Cr, As, Y, Nb, Pb, Th, and except in one sample (13716) for Ga and Rb (Figure 6B).

### 3.3. Discussion

#### 3.3.1. Instrumental Limits

Under the analysis conditions followed in this study, XRD on cohesive samples clearly appears to be less sensitive. Only phases with more than one diffraction peak on powder XRD patterns and phases whose identification is not much dependent on crystal orientation are systematically detected in cohesive samples. The area analyzed when using a conventional diffractometer with a Göbel mirror is sufficiently large as to adequately sample a specimen's heterogeneity in a representative manner. On the contrary, the heterogeneous nature of cohesive samples with coarse inclusions does tend to introduce biases when elemental analyses are carried out on areas smaller than 500 mm<sup>2</sup>. Differences between cohesive and powder samples are lower in EDXS than in PIXE analyses, and this likely relates to the higher number of analyses conducted on each cohesive piece. To summarize, non-invasive XRD analyses in these conditions are less sensitive but still accurate for ochre characterization, while non-invasive EDXS and PIXE analyses require multiple measurements (more than six in our case) in order to overcome the biases introduced by ochre grain-size and mineralogical heterogeneity.

#### 3.3.2. Post-Depositional Alterations

The first surficial post-depositional modification identified from our results was the presence of deposits on the surface of several samples, despite the fact that the surface had been washed. However, the elemental and mineralogical composition of these superficial salts cannot be mistaken with the internal composition of both the shale and ferricrete pieces given they are not present within these two geomaterials. Two other patterns in our results can also be related to post-depositional alterations: (1) kaolinite and quartz are less frequently detected in archeological samples relative to geological samples; (2) Si content is much lower on the surface of all archeological shale pieces (both EDXS and PIXE analyses). This could be due to the formation of a thin coating with a distinct composition on the surface of pieces that have a matrix constituted by clay minerals (shale, phyllite, shale/sandstone), which would potentially cover quartz grains. This layer may have formed within the archeological deposits but may also be a feature inherited from the sub-primary deposits they come from, meaning that already altered pieces may have been introduced into the site. In order to determine the validity of both of these hypotheses, further data would need to be obtained via the analysis of geological shale pieces with a patina. For ferricrete pieces, the presence of a weathering cortex influences the results of XRD surface analyses for both geological and archeological samples, while this same weathering cortex would appear to affect the EDXS results only for archaeological samples. This may indicate that the sub-primary geological cortex has elemental composition that is more or less similar to the center of the piece, albeit with lower degrees of crystallinity. With regard to archeological ferricrete pieces, post-depositional processes likely induced the migration of a part of the elements at the surface of the sub-primary cortex, as was the case for most archeological pieces.

Surprisingly, trace elements seem to be less affected than major elements by alteration processes. We observed differences in trace element contents at the surface of one ochre piece only. The number of trace elements accurately determined by PIXE was, however, quite low in our case (nine elements). Further research is necessary in order to evaluate the role of trace element migration in the formation of secondary patinas in archaeological deposits from Southern African rock shelters, such as at Diepkloof rock shelter.

Additionally, post-depositional processes likely contributed to the differences in iron oxide and oxy-hydroxide identified on the surface of archeological pieces relative to powders. Such differences could stem from one of two effects, either there are differences in detection sensitivity, or mineralogical compositions may truly be distinct. We are inclined to favor this second hypothesis for the following reasons. When differences are perceived, the iron oxides or oxy-hydroxides detected in powders always correspond to lower heat-intensities relative to surface readings (goethite in powder and hematite on sample surface,

maghemite on sample surfaces and hematite in powder). Furthermore, fire features are frequent all over the site sequence [146], and the heat treatment of silcrete has been identified in several stratigraphic units [147,148]. The high quantity of intentional fire use on the site seems more parsimonious therefore with the second of the above-mentioned hypotheses.

### 3.3.3. Consequences for Archeological Inferences

Having now determined both the potential instrumental limits and possible post-depositional alterations, we can now move forward in the construction of a rigorous interpretive framework for our results. Firstly, the two main rock categories observed (shale, including phyllite, and ferricrete) remain clearly distinguishable by their percentages in major elements and by their mineralogical compositions. Interestingly, the absence of clay minerals in cohesive ferricrete pieces allows for consistent identification of ferricrete relative to shale pieces with a clay mineral matrix. However, this particular collection may represent an isolated case study given the salty nature of the superficial coatings of post-depositional origin identified on the archeological pieces and the absence of similar compounds in their internal composition. By comparison, when archeological deposits are rich in clay minerals, sediment adhering to archeological remains may sometimes be difficult to distinguish from the actual surface of a piece of mudstone or shale.

Regarding the identification of geological and geographical origins, it would appear that non-invasive XRD analyses are much more limited seeing as they are unable to detect all families of clay minerals in cohesive samples. Moreover, we cannot use the criteria of illite crystallinity as proposed for powder samples, because the conditions of analyses are not suitable for peak deconvolution [17]. Pyrophyllite, a major proxy for a non-local geological origin was nonetheless clearly detected in one ochre piece. Qualitative SEM-EDXS results can also be used. The micro-structure of the ochre samples allows us to distinguish between true shale (*sensu stricto*), phyllite, and ferricrete, and these are relevant distinctions for determining particular geological origins [28].

Finally, we showed that the contents of six trace elements are not affected by elemental migrations at the surface of archeological samples, among which five are accurately quantified on the surface of geological samples in comparison with homogenized powders: As, Y, Nb, Pb, and Th. This list is quite different from the list of trace elements quantified by ICP-MS that were used to discriminate the geological shale samples, which were As, Ba, Cr, Sb, and V [28]. Moreover, it is quite a low number of trace elements for the discrimination of geological ochre sources in general [18,19,38,39,56,58–61,63,64,85,122]. Nonetheless, the discrimination between two sources based on a few trace elements is possible as soon as these sources are characterized by consistent and significant differences. This might be the case, for instance, if they come from different types of geological formations, as shown by a previous PIXE study [36]. It is also possible to carry out multi-variate analyses on this set of variables in order to make an efficient selection of the trace elements that have the highest weights in inter-source variations. After a careful consideration of the limitations of the PIXE analyses conducted at the surface of heterogeneous ochre pieces (low representativeness of small area PIXE surface analyses for instance), and an evaluation of post-depositional aspects, we can now securely conclude that provenance research using non-invasive PIXE analyses are theoretically possible on this particular collection. Further investigations will be carried out on a larger selection of pieces in the future.

As a whole, we demonstrated that non-invasive analyses can be used to address provenance issues in the Diepkloof ochre collection, though they do not allow for specific attributions to a particular source. Moreover, such methods do not allow determining the geological origin of each single archeological piece. The methodology we employed here in order to enhance the robustness of our inferences should be extended to other contexts when analysts are limited to sacrificing only small numbers of samples for more invasive methods of analyses.

Although evaluating the efficiency of non-invasive analyses to detect the evidence of heat treatment was not part of the initial goals of this project, we did find evidence that

ochre pieces were heated by using non-invasive XRD analyses. The differences observed between the inside and the surface of the analyzed samples favor incidental burning rather than intentional heating [82]. These results were nevertheless very useful for discussions regarding the possibility of heat-treated ochre pieces at the Klasies river main site, as these were analyzed in similar conditions [27].

#### 4. Conclusions

A thorough review of both invasive and non-invasive methods used in ochre studies has shown the degree to which these different approaches can complement one-another. While conventional invasive methods provide more robust and consistent results, some non-invasive or minimally invasive studies do successfully address some aspects of raw material transformation and provenience issues. Our results provide new information on the relevance of non-invasive XRD, SEM-EDXS, and PIXE methods used in ochre characterization. The methodology we followed, which was based on the comparison of invasive and non-invasive analyses of both geological and archeological samples, was particularly useful for demonstrating the respective limitations of these methods and the potential effects of post-depositional processes on the surfaces of archeological specimens. Once these biases were clearly identified, they were considered and were used to temper the final results and the resulting inferences. While these were ultimately less precise due to the aforementioned biases, they nevertheless provided accurate and relevant information on raw material characterization, their provenance, and the question of heat treatment. On the whole, non-invasive XRD analyses appear to be a key method for addressing a broad range of archeological issues with regard to ochre characterization. The qualitative and semi-quantitative results of SEM-EDXS surface analyses were complementary to XRD analyses by adding information on the micro-structure of the pieces and the ranges of composition in major elements.

The methodological results presented here, when combined with other previously published results, provide clear future avenues with regard to how both robust invasive and non-invasive analyses can be combined in order to respond to different lines of archeological questioning. Nonetheless, the relative success of non-invasive methods for the characterization of ochre materials shall not move us away from other avenues of in-depth methodological research as initiated in this work. In particular, taphonomic biases require a more general and broad scale evaluation; minimally invasive methods such as LA-ICP-MS may represent a more optimal compromise relative to non-invasive PIXE analyses given that they are affected by these biases and by instrumental limits related to the analysis of iron-rich matrixes. These represent starting points for methodological improvements in archeological ochre studies at a broader scale.

**Supplementary Materials:** The following are available online at <https://www.mdpi.com/2075-163X/11/2/210/s1>, Table S1: EDXS data compared with ICP-OES (major) data for 5 geologic samples (powder pellets), Table S2: Comparison of PIXE data with ICP-OES (major) and ICP-MS (traces) results for 5 geologic samples (powder pellets), Table S3: Detailed results of SEM-EDXS analyses of archeological samples (surface and section), Table S4: Detailed results of PIXE analyses of archaeological samples (surface and section).

**Funding:** Région Aquitaine, France: Prehistoric ochre project.

**Institutional Review Board Statement:** Not applicable.

**Informed Consent Statement:** Not applicable.

**Data Availability Statement:** Not applicable.

**Acknowledgments:** The author wishes to thank Floréal Danieal (IRAMAT-CRP2A), Pierre-Jean Texier, and Pierre Guibert for the supervision of the PhD thesis from which part of the results presented here come from. Thank you to Stéphane Dubernet and Nadia Cantin for their advice on XRD acquisition; to Yannick Lefrais for his advice in SEM-EDXS analyses; to Lucile Beck, Laurent Pichon and Claire Pacheco (C2RMF) for their advice and help in PIXE analyses at the AGLAE platform; and

to John Parkington and Judith Sealy (University of Cape Town) for their help with the export permit application. We are also grateful to the French Ministry of Foreign Affairs (MAE), the Aquitaine region, the Provence-Alpes-Côte-d'Azur region, and the Centre National de la Recherche Scientifique (CNRS) for their financial support of the Diepkloof excavations. This ochre characterization project was funded by the University of Bordeaux 3, the Centre National de la Recherche Scientifique, and the Région Aquitaine, France.

**Conflicts of Interest:** The author declares no conflict of interest.

## References

- Brooks, A.S.; Yellen, J.E.; Potts, R.; Behrensmeier, A.K.; Deino, A.L.; Leslie, D.E.; Ambrose, S.H.; Ferguson, J.R.; d'Errico, F.; Zipkin, A.M.; et al. Long-Distance Stone Transport and Pigment Use in the Earliest Middle Stone Age. *Science* **2018**, *360*, 90–94. [[CrossRef](#)] [[PubMed](#)]
- Barham, L.S. Systematic Pigment Use in the Middle Pleistocene of South-Central Africa. *Curr. Anthropol.* **2002**, *43*, 181–190. [[CrossRef](#)]
- Mcbrearty, S.; Brooks, A.S. The Revolution That Wasn't: A New Interpretation of the Origin of Modern Human Behavior. *J. Hum. Evol.* **2000**, *39*, 453–563. [[CrossRef](#)] [[PubMed](#)]
- Roebroeks, W.; Sier, M.J.; Nielsen, T.K.; De Loecker, D.; Parés, J.M.; Arps, C.E.S.; Múcher, H.J. Use of Red Ochre by Early Neandertals. *Proc. Natl. Acad. Sci. USA* **2012**, *109*, 1889–1894. [[CrossRef](#)] [[PubMed](#)]
- Watts, I.; Chazan, M.; Wilkins, J. Early Evidence for Brilliant Ritualized Display: Specularite Use in the Northern Cape (South Africa) between ~500 and ~300 Ka. *Curr. Anthropol.* **2016**, *57*, 287–310. [[CrossRef](#)]
- Audouin, F.; Plisson, H. Les Ogres et Leurs Témoins Au Paléolithique En France: Enquête et Expériences Sur Leur Validité Archéologique. *Cah. Cent. Rech. Préhistoriques* **1982**, *8*, 33–80.
- Philibert, S. L'ocre et Le Traitement Des Peaux: Révision d'une Conception Traditionnelle Par l'analyse Fonctionnelle Des Grattoirs Ocrés de La Balma Magineda (Andorre). *L'Anthropologie* **1994**, *98*, 447–453.
- Rifkin, R.F. Assessing the Efficacy of Red Ochre as a Prehistoric Hide Tanning Ingredient. *J. Afr. Archaeol.* **2011**, *9*, 131–158. [[CrossRef](#)]
- Rifkin, R.F. Ethnographic and Experimental Perspectives on the Efficacy of Ochre as a Mosquito Repellent. *S. Afr. Archaeol. Bull.* **2015**, *70*, 64–75.
- Rifkin, R.F.; Dayet, L.; Queffelec, A.; Summers, B.; Lategan, M.; d'Errico, F. Evaluating the Photoprotective Effects of Ochre on Human Skin by In Vivo SPF Assessment: Implications for Human Evolution, Adaptation and Dispersal. *PLoS ONE* **2015**, *10*, e0136090. [[CrossRef](#)] [[PubMed](#)]
- Rudner, I.E. *Khoisan Pigments and Paints and Their Relationship to Rock Paintings*; South African Museum: Cape Town, South Africa, 1982.
- Wadley, L. Putting Ochre to the Test: Replication Studies of Adhesives That May Have Been Used for Hafting Tools in the Middle Stone Age. *J. Hum. Evol.* **2005**, *49*, 587–601. [[CrossRef](#)] [[PubMed](#)]
- Wadley, L.; Williamson, B.; Lombard, M. Ochre in Hafting in Middle Stone Age Southern Africa: A Practical Role. *Antiquity* **2004**, *78*, 661–675. [[CrossRef](#)]
- White, R. Actes de Substance: De La Matière Au Sens Dans La Représentation Paléolithique. *Techné* **1996**, *3*, 29–38.
- Cornell, R.; Schwertmann, U. *The Iron Oxides: Structure, Properties, Reactions, Occurrences and Uses*; Wiley: Weinheim, Germany, 2003.
- Cavallo, G.; Fontana, F.; Gonzato, F.; Peresani, M.; Riccardi, M.P.; Zorzin, R. Textural, Microstructural, and Compositional Characteristics of Fe-Based Geomaterials and Upper Paleolithic Ocher in the Lessini Mountains, Northeast Italy: Implications for Provenance Studies. *Geoarchaeology* **2017**, *32*, 437–455. [[CrossRef](#)]
- Dayet, L.; Bourdonnec, F.-X.L.; Daniel, F.; Porraz, G.; Texier, P.-J. Ochre Provenance and Procurement Strategies during The Middle Stone Age at Diepkloof Rock Shelter, South Africa. *Archaeometry* **2016**, *58*, 807–829. [[CrossRef](#)]
- MacDonald, B.L.; Hancock, R.G.V.; Cannon, A.; Pidruczny, A. Geochemical Characterization of Ochre from Central Coastal British Columbia, Canada. *J. Archaeol. Sci.* **2011**, *38*, 3620–3630. [[CrossRef](#)]
- MacDonald, B.L.; Fox, W.; Dubreuil, L.; Beddard, J.; Pidruczny, A. Iron Oxide Geochemistry in the Great Lakes Region (North America): Implications for Ochre Provenance Studies. *J. Archaeol. Sci. Rep.* **2018**, *19*, 476–490. [[CrossRef](#)]
- Rifkin, R.F. Processing Ochre in the Middle Stone Age: Testing the Inference of Prehistoric Behaviours from Actualistically Derived Experimental Data. *J. Anthropol. Archaeol.* **2012**, *31*, 174–195. [[CrossRef](#)]
- Watts, I. Ochre in the Middle Stone Age of Southern Africa: Ritualised Display or Hide Preservative? *S. Afr. Archaeol. Bull.* **2002**, *57*, 1–14. [[CrossRef](#)]
- Couraud, C. Pigments Utilisés En Préhistoire, Provenance, Préparation, Mode d'utilisation. *L'Anthropologie* **1988**, *92*, 17–28.
- Watts, I. The Pigments from Pinnacle Point Cave 13B, Western Cape, South Africa. *J. Hum. Evol.* **2010**, *59*, 392–411. [[CrossRef](#)]
- Hovers, E.; Ilani, S.; Bar-Yosef, O.; Vandermeersch, B. An Early Case of Color Symbolism: Ochre Use by Modern Humans in Qafzeh Cave. *Curr. Anthropol.* **2003**, *44*, 491–522. [[CrossRef](#)]
- Salomon, H. *Les Matières Colorantes Au Début Du Paléolithique Supérieur: Sources, Transformations et Fonctions*; Université Bordeaux 1: Bordeaux, France, 2009.

26. Hodgskiss, T. An Investigation into the Properties of the Ochre from Sibudu, KwaZulu-Natal, South Africa. *S. Afr. Humanit.* **2012**, *24*, 99–120.
27. Dayet Bouillot, L.; Wurz, S.; Daniel, F. Ochre Resources, Behavioural Complexity and Regional Patterns in the Howiesons Poort: New Insights from Klasies River Main Site, South Africa. *J. Afr. Archaeol.* **2017**, *15*, 20–41. [[CrossRef](#)]
28. Dayet, L.; Texier, P.-J.; Daniel, F.; Porraz, G. Ochre Resources from the Middle Stone Age Sequence of Diepkloof Rock Shelter, Western Cape, South Africa. *J. Archaeol. Sci.* **2013**, *40*, 3492–3505. [[CrossRef](#)]
29. Dayet, L.; Faivre, J.-P.; Le Bourdonnec, F.-X.; Discamps, E.; Royer, A.; Claud, E.; Lahaye, C.; Cantin, N.; Tartar, E.; Queffelec, A.; et al. Manganese and Iron Oxide Use at Combe-Grenal (Dordogne, France): A Proxy for Cultural Change in Neanderthal Communities. *J. Archaeol. Sci. Rep.* **2019**, *25*, 239–256. [[CrossRef](#)]
30. Rosso, D.E.; d’Errico, F.; Queffelec, A. Patterns of Change and Continuity in Ochre Use during the Late Middle Stone Age of the Horn of Africa: The Porc-Epic Cave Record. *PLoS ONE* **2017**, *12*, e0177298. [[CrossRef](#)]
31. Rosso, D.E.; d’Errico, F.; Zilhão, J. Stratigraphic and Spatial Distribution of Ochre and Ochre Processing Tools at Porc-Epic Cave, Dire Dawa, Ethiopia. *Quat. Int.* **2014**, *343*, 85–99. [[CrossRef](#)]
32. Cavallo, G.; Fontana, F.; Gialanella, S.; Gonzato, F.; Riccardi, M.P.; Zorzin, R.; Peresani, M. Heat Treatment of Mineral Pigment During the Upper Palaeolithic in North-East Italy. *Archaeometry* **2018**, *60*, 1045–1061. [[CrossRef](#)]
33. Mauran, G.; Lebon, M.; Lapauze, O.; Nankela, A.; Détroit, F.; Lesur, J.; Bahain, J.-J.; Pleurdeau, D. Archaeological Ochres of the Rock Art Site of Leopard Cave (Erongo, Namibia): Looking for Later Stone Age Sociocultural Behaviors. *Afr. Archaeol. Rev.* **2020**, *37*, 527–550. [[CrossRef](#)]
34. Fiore, D.; Maier, M.; Parera, S.D.; Orquera, L.; Piana, E. Chemical Analyses of the Earliest Pigment Residues from the Uttermost Part of the Planet (Beagle Channel Region, Tierra Del Fuego, Southern South America). *J. Archaeol. Sci.* **2008**, *35*, 3047–3056. [[CrossRef](#)]
35. Salomon, H.; Vignaud, C.; Coquinot, Y.; Pagès-Camagna, S.; Pomiès, M.-P.; Geneste, J.-M.; Menu, M.; Julien, M.; David, F. Les matières colorantes au début du Paléolithique supérieur: Caractérisation chimique et structurale, transformation et valeur symbolique. In *Techné Hors-Série*; Center for Research and Restoration of the Museums of France: Paris, France, 2008; pp. 17–23.
36. Mathis, F.; Bodu, P.; Dubreuil, O.; Salomon, H. PIXE Identification of the Provenance of Ferruginous Rocks Used by Neanderthals. *Nucl. Instrum. Methods Phys. Res. Sect. B Beam Interact. Mater. At.* **2014**, *331*, 275–279. [[CrossRef](#)]
37. Pradeau, J.-V.; Binder, D.; Vérati, C.; Lardeaux, J.-M.; Dubernet, S.; Lefrais, Y.; Regert, M. Procurement Strategies of Neolithic Colouring Materials: Territoriality and Networks from 6th to 5th Millennia BCE in North-Western Mediterranean. *J. Archaeol. Sci.* **2016**, *71*, 10–23. [[CrossRef](#)]
38. Zipkin, A.M.; Hanchar, J.M.; Brooks, A.S.; Grabowski, M.W.; Thompson, J.C.; Gomani-Chindebvu, E. Ochre Fingerprints: Distinguishing among Malawian Mineral Pigment Sources with Homogenized Ochre Chip LA-ICPMS. *Archaeometry* **2015**, *57*, 297–317. [[CrossRef](#)]
39. Zipkin, A.M.; Ambrose, S.H.; Lundstrom, C.C.; Bartov, G.; Dwyer, A.; Taylor, A.H. Red Earth, Green Glass, and Compositional Data: A New Procedure for Solid-State Elemental Characterization, Source Discrimination, and Provenience Analysis of Ochres. *J. Archaeol. Method Theory* **2020**, *27*, 930–970. [[CrossRef](#)]
40. Watts, I. Red ochre, body-painting, and language: Interpreting the Blombos ochre. In *The Cradle of Language*; Botha, R., Knight, C., Eds.; Oxford University Press: Oxford, UK, 2009; pp. 62–92, ISBN 978-0-19-954586-5.
41. D’Errico, F.; Salomon, H.; Vignaud, C.; Stringer, C. Pigments from the Middle Palaeolithic Levels of Es-Skhul (Mount Carmel, Israel). *J. Archaeol. Sci.* **2010**, *37*, 3099–3110. [[CrossRef](#)]
42. Henshilwood, C.S.; d’Errico, F.; van Niekerk, K.L.; Coquinot, Y.; Jacobs, Z.; Lauritzen, S.-E.; Menu, M.; García-Moreno, R. A 100,000-Year-Old Ochre-Processing Workshop at Blombos Cave, South Africa. *Science* **2011**, *334*, 219–222. [[CrossRef](#)]
43. Gialanella, S.; Belli, R.; Dalmeri, G.; Lonardelli, I.; Mattarelli, M.; Montagna, M.; Toniutti, L. Artificial or Natural Origin of Hematite-Based Red Pigments in Archaeological Contexts: The Case of Riparo Dalmeri (Trento, Italy). *Archaeometry* **2011**, *53*, 950–962. [[CrossRef](#)]
44. Moyo, S.; Mphuthi, D.; Cukrowska, E.; Henshilwood, C.S.; van Niekerk, K.; Chimuka, L. Blombos Cave: Middle Stone Age Ochre Differentiation through FTIR, ICP OES, ED XRF and XRD. *Quat. Int.* **2016**, *404*, 20–29. [[CrossRef](#)]
45. Garilli, V.; Vita, G.; La Parola, V.; Pinto Vraca, M.; Giarrusso, R.; Rosina, P.; Bonfiglio, L.; Sineo, L. First Evidence of Pleistocene Ochre Production from Bacteriogenic Iron Oxides. A Case Study of the Upper Palaeolithic Site at the San Teodoro Cave (Sicily, Italy). *J. Archaeol. Sci.* **2020**, *123*, 105221. [[CrossRef](#)]
46. MacDonald, B.L.; Chatters, J.C.; Reinhardt, E.G.; Devos, F.; Meacham, S.; Rissolo, D.; Rock, B.; Maillot, C.L.; Stalla, D.; Marino, M.D.; et al. Paleindian Ochre Mines in the Submerged Caves of the Yucatán Peninsula, Quintana Roo, Mexico. *Sci. Adv.* **2020**, *6*, eaba1219. [[CrossRef](#)] [[PubMed](#)]
47. Goemaere, E.; Salomon, H.; Billard, C.; Querré, G.; MATHIS, F.; Golitko, M.; Dubrulle-Brunaud, C.; Savary, X.; Dreesen, R. Les Hématites Oolithiques Du Néolithique Ancien et Du Mésolithique de Basse-Normandie (France): Caractérisation Physico-Chimique et Recherche Des Provenances. *Anthropol. Praehist.* **2016**, *125*, 89–119.
48. Tortosa, J.E.A.; Gallello, G.; Roldán, C.; Cavallo, G.; Pastor, A.; Murcia-Mascarós, S. Characterization and Sources of Paleolithic–Mesolithic Ochre from Coves de Santa Maira (Valencian Region, Spain). *Geoarchaeology* **2021**, *36*, 72–91. [[CrossRef](#)]
49. Matarrese, A.; Di Prado, V.; Poiré, D.G. Petrologic Analysis of Mineral Pigments from Hunter-Gatherers Archaeological Contexts (Southeastern Pampean Region, Argentina). *Quat. Int.* **2011**, *245*, 2–12. [[CrossRef](#)]

50. Zilhão, J.; Angelucci, D.E.; Badal-García, E.; d’Errico, F.; Daniel, F.; Dayet, L.; Douka, K.; Higham, T.F.G.; Martínez-Sánchez, M.J.; Montes-Bernárdez, R.; et al. Symbolic Use of Marine Shells and Mineral Pigments by Iberian Neandertals. *Proc. Natl. Acad. Sci. USA* **2010**, *107*, 1023–1028. [[CrossRef](#)] [[PubMed](#)]
51. Darchuk, L.; Tsybrii, Z.; Worobiec, A.; Vázquez, C.; Palacios, O.M.; Stefaniak, E.A.; Gatto Rotondo, G.; Sizov, F.; Van Grieken, R. Argentinean Prehistoric Pigments’ Study by Combined SEM/EDX and Molecular Spectroscopy. *Spectrochim. Acta. A Mol. Biomol. Spectrosc.* **2010**, *75*, 1398–1402. [[CrossRef](#)]
52. Lebon, M.; Gallet, X.; Bondetti, M.; Pont, S.; Mauran, G.; Walter, P.; Bellot-Gurlet, L.; Puaud, S.; Zazzo, A.; Forestier, H.; et al. Characterization of Painting Pigments and Ochres Associated with the Hoabinhian Archaeological Context at the Rock-Shelter Site of Doi Pha Kan (Thailand). *J. Archaeol. Sci. Rep.* **2019**, *26*, 101855. [[CrossRef](#)]
53. Wojcieszak, M.; Wadley, L. Raman Spectroscopy and Scanning Electron Microscopy Confirm Ochre Residues on 71 000-Year-Old Bifacial Tools from Sibudu, South Africa. *Archaeometry* **2018**, *60*, 1062–1076. [[CrossRef](#)]
54. Wojcieszak, M.; Wadley, L. A Raman Micro-Spectroscopy Study of 77,000 to 71,000 Year Old Ochre Processing Tools from Sibudu, KwaZulu-Natal, South Africa. *Herit. Sci.* **2019**, *7*, 24. [[CrossRef](#)]
55. Rosso, D.E.; Martí, A.P.; d’Errico, F. Middle Stone Age Ochre Processing and Behavioural Complexity in the Horn of Africa: Evidence from Porc-Epic Cave, Dire Dawa, Ethiopia. *PLoS ONE* **2016**, *11*, e0164793. [[CrossRef](#)]
56. Popelka-Filcoff, R.S.; Robertson, J.D.; Glascock, M.D.; Descantes, C. Trace Element Characterization of Ochre from Geological Sources. *J. Radioanal. Nucl. Chem.* **2007**, *272*, 17–27. [[CrossRef](#)]
57. Popelka-Filcoff, R.S.; Craig, N.; Glascock, M.D.; Robertson, J.D.; Aldenderfer, M.; Speakman, R.J. Instrumental Neutron Activation Analysis of Ochre Artifacts from Jiskairumoko, Peru. In *Archaeological Chemistry*; ACS Symposium Series; American Chemical Society: Washington, DC, USA, 2007; Volume 968, pp. 480–505, ISBN 978-0-8412-7413-6.
58. Popelka-Filcoff, R.S.; Lenehan, C.E.; Glascock, M.D.; Bennett, J.W.; Stopic, A.; Quinton, J.S.; Pring, A.; Walshe, K. Evaluation of Relative Comparator and K0-NAA for Characterization of Aboriginal Australian Ochre. *J. Radioanal. Nucl. Chem.* **2012**, *291*, 19–24. [[CrossRef](#)]
59. Eiselt, B.S.; Popelka-Filcoff, R.S.; Darling, J.A.; Glascock, M.D. Hematite Sources and Archaeological Ochres from Hohokam and O’odham Sites in Central Arizona: An Experiment in Type Identification and Characterization. *J. Archaeol. Sci.* **2011**, *38*, 3019–3028. [[CrossRef](#)]
60. Attard Montalto, N.; Shortland, A.; Rogers, K. The Provenancing of Ochres from the Neolithic Temple Period in Malta. *J. Archaeol. Sci.* **2012**, *39*, 1094–1102. [[CrossRef](#)]
61. Domingo, I.; García-Borja, P.; Roldán, C. Identification, Processing and Use of Red Pigments (Hematite and Cinnabar) in the Valencian Early Neolithic (Spain). *Archaeometry* **2012**, *54*, 868–892. [[CrossRef](#)]
62. Scadding, R.; Winton, V.; Brown, V. An LA-ICP-MS Trace Element Classification of Ochres in the Weld Range Environ, Mid West Region, Western Australia. *J. Archaeol. Sci.* **2015**, *54*, 300–312. [[CrossRef](#)]
63. Zarzycka, S.E.; Surovell, T.A.; Mackie, M.E.; Pelton, S.R.; Kelly, R.L.; Goldberg, P.; Dewey, J.; Kent, M. Long-Distance Transport of Red Ocher by Clovis Foragers. *J. Archaeol. Sci. Rep.* **2019**, *25*, 519–529. [[CrossRef](#)]
64. Pierce, D.E.; Wright, P.J.; Popelka-Filcoff, R.S. Seeing Red: An Analysis of Archeological Hematite in East Central Missouri. *Archaeol. Anthropol. Sci.* **2020**, *12*, 23. [[CrossRef](#)]
65. Trabska, J.; Walanus, A.; Ciesielczuk, J.; Samek, L.; Dutkiewicz, E. Ferruginous Raw Material Sources for Palaeolithic in Poland? Promising Results of Provenance Studies. In Proceedings of the 9th International Conference on NDT of Art 2008, Jerusalem, Israel, 25–30 May 2008; pp. 1–8.
66. Young, T. Appendix 5, Geochemical analysis of ferruginous materials from Twin Rivers. In *The Middle Stone Age of Zambia, Southcentral Africa*; Barham, L.S., Ed.; University of Bristol: Bristol, UK, 2000; p. 26572.
67. Beck, L.; Salomon, H.; Lahlil, S.; Lebon, M.; Odin, G.P.; Coquinot, Y.; Pichon, L. Non-Destructive Provenance Differentiation of Prehistoric Pigments by External PIXE. *Nucl. Instrum. Methods Phys. Res. Sect. B Beam Interact. Mater. At.* **2012**, *273*, 173–177. [[CrossRef](#)]
68. Belli, R.; Lonardelli, I.; Quaranta, A.; Girardi, F.; Cusinato, A.; Dalmeri, G. A methodological approach to discriminate between natural and synthetic haematite used as prehistoric pigments: Preliminary results (Riparo Dalmeri—Trentino, Italy). In Proceedings of the Conference of the Associazione Italiana di Archeometria, Firenze 2007, Patron Editore, Bologna, Italy, 26–29 February 2008; pp. 179–185.
69. Bernatchez, J.A. Geochemical Characterization of Archaeological Ochre at Nelson Bay Cave (Western Cape Province), South Africa. *S. Afr. Archaeol. Bull.* **2008**, *63*, 3–11. [[CrossRef](#)]
70. Cavallo, G.; Fontana, F.; Gonzato, F.; Guerreschi, A.; Riccardi, M.P.; Sardelli, G.; Zorzini, R. Sourcing and Processing of Ochre during the Late Upper Palaeolithic at Tagliente Rock-Shelter (NE Italy) Based on Conventional X-Ray Powder Diffraction Analysis. *Archaeol. Anthropol. Sci.* **2017**, *9*, 763–775. [[CrossRef](#)]
71. Cavallo, G.; Riccardi, M.P.; Zorzini, R. Powder Diffraction of Yellow and Red Natural Earths from Lessini Mountains in NE Italy. *Powder Diffr.* **2015**, *30*, 122–129. [[CrossRef](#)]
72. Salomon, H.; Vignaud, C.; Coquinot, Y.; Beck, L.; Stringer, C.; Strivay, D.; D’errico, F. Selection and Heating of Colouring Materials in the Mousterian Level of Es-Skhul (ca. 100 000 Years BP, Mount Carmel, Israel). *Archaeometry* **2012**, *54*, 698–722. [[CrossRef](#)]
73. D’Errico, F.; García Moreno, R.; Rifkin, R.F. Technological, Elemental and Colorimetric Analysis of an Engraved Ochre Fragment from the Middle Stone Age Levels of Klasies River Cave 1, South Africa. *J. Archaeol. Sci.* **2012**, *39*, 942–952. [[CrossRef](#)]

74. Dayet, L.; Daniel, F.; Guibert, P.; Texier, P.-J. Non-Destructive Analysis of Archaeological Ochre: A Preliminary Application to the Middle Stone Age Site of Diepkloof Rock Shelter (South Africa). *Open J. Archaeom.* **2013**, *1*, e19. [[CrossRef](#)]
75. Dayet, L.; d'Errico, F.; Garcia-Moreno, R. Searching for Consistencies in Châtelperronian Pigment Use. *J. Archaeol. Sci.* **2014**, *44*, 180–193. [[CrossRef](#)]
76. Godfrey-Smith, D.I.; Ilani, S. Past Thermal History of Goethite and Hematite Fragments from Qafzeh Cave Deduced from Thermal Activation Characteristics of the 110 °C TL Peak of Enclosed Quartz Grains. *Archéosci. Rev. Archéom.* **2004**, *28*, 185–190. [[CrossRef](#)]
77. Goemaere, E.; Salomon, H.; Querré, G.; MATHIS, F.; Dreesen, R.; Hamon, C.; Constantin, C.; Dominique, B.; Wijnen, J.; Jadin, I. Caractérisation Physico-Chimique et Recherche Des Provenances Des Hématites Oolithiques Des Sites Du Néolithique Ancien de Hesbaye (Province de Liège, Belgique) et Des Sites Néolithiques Des Sources de La Dendre (Province Du Hainaut, Belgique). *Anthropol. Praehist.* **2016**, *125*, 153–191.
78. Hughes, J.C.; Solomon, A. A Preliminary Study of Ochres and Pigmentaceous Materials from KwaZulu-Natal, South Africa: Towards an Understanding of San Pigment and Paint Use. *S. Afr. Humanit.* **2000**, *12*, 15–31.
79. Macdonald, B.L.; Hancock, R.G.V.; Cannon, A.; McNeill, F.; Reimer, R.; Pidruczny, A. Elemental Analysis of Ochre Outcrops in Southern British Columbia, Canada. *Archaeometry* **2013**, *55*, 1020–1033. [[CrossRef](#)]
80. Di Prado, V.S.; Scalice, R.; Poire, D.G.; Canalicchio, J.; Gómez Peral, L. *Análisis de los Elementos Colorantes Provenientes del Sitio Calera (Sierras Bayas, Región Pampeana). Una Exploración del uso Social y Ritual de los Pigmentos*; Sociedad Argentina de Antropología: Buenos Aires, Argentina, 2007; ISBN 978-987-1280-07-0.
81. Mooney, S.D.; Geiss, C.; Smith, M.A. The Use of Mineral Magnetic Parameters to Characterize Archaeological Ochres. *J. Archaeol. Sci.* **2003**, *30*, 511–523. [[CrossRef](#)]
82. Salomon, H.; Vignaud, C.; Lahlil, S.; Menguy, N. Solutrean and Magdalenian Ferruginous Rocks Heat-Treatment: Accidental and/or Deliberate Action? *J. Archaeol. Sci.* **2015**, *55*, 100–112. [[CrossRef](#)]
83. San Juan-Foucher, C. Étude typotechnologique, fonctionnelle et spatiale des matières colorantes du Bois-Ragot. Niveaux magdaléniens et aziliens. In *Mémoires de la Société Préhistorique Française*; Chollet, A., Dujardin, V., Eds.; French Prehistoric Society: Rennes, France, 2005; Volume 38, pp. 261–274.
84. Pomiès, M.-P.; Vignaud, C. Analyses de pigments provenant du site de Bois-Ragot: Diffraction Rx et observation en MET, La grotte du Bois-Ragot à Gouex (Vienne), Magdalénien et Azilien, essais sur les hommes et leur environnement. In *Mémoires de la Société Préhistorique Française*; Chollet, A., Dujardin, V., Eds.; French Prehistoric Society: Rennes, France, 2005; Volume 38, pp. 275–278.
85. Velliky, E.C.; MacDonald, B.L.; Porr, M.; Conard, N.J. First Large-Scale Provenance Study of Pigments Reveals New Complex Behavioural Patterns during the Upper Palaeolithic of South-Western Germany. *Archaeometry* **2020**, *63*, 173–193. [[CrossRef](#)]
86. Velliky, E.C.; Barbieri, A.; Porr, M.; Conard, N.J.; MacDonald, B.L. A Preliminary Study on Ochre Sources in Southwestern Germany and Its Potential for Ochre Provenance during the Upper Paleolithic. *J. Archaeol. Sci. Rep.* **2019**, *27*, 101977. [[CrossRef](#)]
87. Wadley, L. Cemented Ash as a Receptacle or Work Surface for Ochre Powder Production at Sibudu, South Africa, 58,000 Years Ago. *J. Archaeol. Sci.* **2010**, *37*, 2397–2406. [[CrossRef](#)]
88. De Faria, D.L.; Venâncio Silva, S.; De Oliveira, M.T. Raman microspectroscopy of some iron oxides and oxyhydroxides. *J. Raman Spectrosc.* **1997**, *28*, 873–878. [[CrossRef](#)]
89. Loudon, J.D. Raman Microscopy. In *Practical Raman Spectroscopy*; Gardiner, D.J., Graves, P.R., Eds.; Springer: Berlin/Heidelberg, Germany, 1989; pp. 119–151, ISBN 978-3-642-74040-4.
90. Newbury, D.E. Microbeam Analysis of Samples of Unusual Shape. *J. Phys. Colloq.* **1984**, *45*, 775–780. [[CrossRef](#)]
91. Potts, P.J.; Webb, P.C.; Williams-Thorpe, O. Investigation of a Correction Procedure for Surface Irregularity Effects Based on Scatter Peak Intensities in the Field Analysis of Geological and Archaeological Rock Samples by Portable X-Ray Fluorescence Spectrometry. *J. Anal. At. Spectrom.* **1997**, *12*, 769–776. [[CrossRef](#)]
92. Potts, P.J.; West, M. *Portable X-Ray Fluorescence Spectrometry*; Royal Society of Chemistry: Cambridge, UK, 2008; ISBN 978-0-85404-552-5.
93. Pouchou, J.-L.; Pichoir, F. Quantitative Analysis of Homogeneous or Stratified Microvolumes Applying the Model “PAP”. In *Electron Probe Quantitation*; Heinrich, K.F.J., Newbury, D.E., Eds.; Springer: Boston, MA, USA, 1991; pp. 31–75, ISBN 978-1-4899-2617-3.
94. Pouchou, J.-L. Les méthodes de quantification en microanalyse X. In *Microscopie Electronique à Balayage et Microanalyses*; Brisset, F., Ed.; EDP Sciences: Les Ulis, France, 2008.
95. Calligaro, T.; Dran, J.-C.; Salomon, J. Chapter 5 Ion beam microanalysis. In *Comprehensive Analytical Chemistry; Non-Destructive Microanalysis of Cultural Heritage Materials*; Elsevier: Amsterdam, the Netherlands, 2004; Volume 42, pp. 227–276.
96. Brisset, F.; Boivin, D. L'analyse EDS. In *Microscopie Electronique à Balayage et Microanalyses*; Brisset, F., Ed.; EDP Sciences: Les Ulis, France, 2008.
97. Beck, L.; Lebon, M.; Pichon, L.; Menu, M.; Chiotti, L.; Nespoulet, R.; Paillet, P. PIXE Characterisation of Prehistoric Pigments from Abri Pataud (Dordogne, France). *X-Ray Spectrom.* **2011**, *40*, 219–223. [[CrossRef](#)]
98. Pollard, A.M.; Batt, C.M.; Stern, B.; Young, S.M.M. *Analytical Chemistry in Archaeology*; Cambridge University Press: Cambridge, UK, 2007; ISBN 978-0-521-65572-9.
99. Pollard, A.M.; Heron, C. *Archaeological Chemistry*; Royal Society of Chemistry: London, UK, 2015; ISBN 978-1-78262-611-4.

100. Kanngießner, B.; Haschke, M.; Simionovici, A.; Chevallier, P.; Strelci, C.; Wobrauschek, P.; Fabry, L.; Pahlke, S.; Comin, F.; Barrett, R.; et al. Methodological Developments and Applications. In *Handbook of Practical X-Ray Fluorescence Analysis*; Beckhoff, B., Kanngießner, B., Langhoff, N., Wedell, R., Wolff, H., Eds.; Springer: Berlin/Heidelberg, Germany, 2006; pp. 433–833, ISBN 978-3-540-36722-2.
101. Potts, P.J.; Williams-Thorpe, O.; Webb, P.C. The Bulk Analysis of Silicate Rocks by Portable X-Ray Fluorescence: Effect of Sample Mineralogy in Relation to the Size of the Excited Volume. *Geostand. Newsl.* **1997**, *21*, 29–41. [[CrossRef](#)]
102. Mantler, M.; Willis, J.; Lachance, G.; Vrebos, B.A.R.; Mauser, K.-E.; Kawahara, N.; Rousseau, R.M.; Brouwer, P.N. Quantitative Analysis. In *Handbook of Practical X-Ray Fluorescence Analysis*; Beckhoff, B., Kanngießner, B., Langhoff, N., Wedell, R., Wolff, H., Eds.; Springer: Berlin/Heidelberg, Germany, 2006; pp. 309–410, ISBN 978-3-540-36722-2.
103. Speakman, R.J.; Shackley, M.S. Silo Science and Portable XRF in Archaeology: A Response to Frahm. *J. Archaeol. Sci.* **2013**, *40*, 1435–1443. [[CrossRef](#)]
104. Flemming, R.L. Micro X-Ray Diffraction (MXRD): A Versatile Technique for Characterization of Earth and Planetary Materials. *Can. J. Earth Sci.* **2007**, *44*, 1333–1346. [[CrossRef](#)]
105. Waseda, Y.; Matsubara, E.; Shinoda, K. Diffraction from Polycrystalline Samples and Determination of Crystal Structure. In *X-ray Diffraction Crystallography: Introduction, Examples and Solved Problems*; Waseda, Y., Matsubara, E., Shinoda, K., Eds.; Springer: Berlin/Heidelberg, Germany, 2011; pp. 107–167, ISBN 978-3-642-16635-8.
106. Moore, D.M.; Reynolds, J.R.C. *X-Ray Diffraction and the Identification and Analysis of Clay Minerals*; Oxford University Press: New York, NY, USA, 1989.
107. Meunier, A. *Les Argiles; Collection Géosciences; Scientifiques GB*; Contemporary Publishing International-GB Science Publisher, Impr.: Paris, France, 2002.
108. Krishnan, K.; Hill, S.L. 3—FT-IR Microsampling Techniques. In *Practical Fourier Transform Infrared Spectroscopy*; Ferraro, J.R., Krishnan, K., Eds.; Academic Press: Cambridge, MA, USA, 1990; pp. 103–165, ISBN 978-0-12-254125-4.
109. Bruno, T.J. Sampling Accessories for Infrared Spectrometry. *Appl. Spectrosc. Rev.* **1999**, *34*, 91–120. [[CrossRef](#)]
110. Miliani, C.; Rosi, F.; Daveri, A.; Brunetti, B.G. Reflection Infrared Spectroscopy for the Non-Invasive in Situ Study of Artists' Pigments. *Appl. Phys. A* **2012**, *106*, 295–307. [[CrossRef](#)]
111. Fabbri, M.; Picollo, M.; Porcinai, S.; Bacci, M. Mid-Infrared Fiber-Optics Reflectance Spectroscopy: A Noninvasive Technique for Remote Analysis of Painted Layers. Part I: Technical Setup. *Appl. Spectrosc.* **2001**, *55*, 420–427. [[CrossRef](#)]
112. Velliky, E.C.; Porr, M.; Conard, N.J. Ochre and Pigment Use at Hohle Fels Cave: Results of the First Systematic Review of Ochre and Ochre-Related Artefacts from the Upper Palaeolithic in Germany. *PLoS ONE* **2018**, *13*, e0209874. [[CrossRef](#)]
113. Hodgskiss, T.; Wadley, L. How People Used Ochre at Rose Cottage Cave, South Africa: Sixty Thousand Years of Evidence from the Middle Stone Age. *PLoS ONE* **2017**, *12*, e0176317. [[CrossRef](#)]
114. Beauvais, A.; Colin, F. Formation and Transformation Processes of Iron Duricrust Systems in Tropical Humid Environment. *Chem. Geol.* **1993**, *106*, 77–101. [[CrossRef](#)]
115. Putzolu, F.; Abad, I.; Balassone, G.; Boni, M.; Cappelletti, P.; Graziano, S.F.; Maczurad, M.; Mondillo, N.; Najorka, J.; Santoro, L. Parent Rock and Climatic Evolution Control on the Genesis of Ni-Bearing Clays in Ni-Co Laterites: New Inferences from the Wingellina Deposit (Western Australia). *Ore Geol. Rev.* **2020**, *120*, 103431. [[CrossRef](#)]
116. Kiehn, A.V.; Brook, G.A.; Glascock, M.D.; Dake, J.Z.; Robbins, L.H.; Campbell, A.C.; Murphy, M.L. Fingerprinting Specular Hematite from Mines in Botswana, Southern Africa. In *Archaeological Chemistry*; ACS Symposium Series; American Chemical Society: Washington, DC, USA, 2007; Volume 968, pp. 460–479, ISBN 978-0-8412-7413-6.
117. Popelka-Filcoff, R.S.; Miksa, E.J.; Robertson, J.D.; Glascock, M.D.; Wallace, H. Elemental Analysis and Characterization of Ochre Sources from Southern Arizona. *J. Archaeol. Sci.* **2008**, *35*, 752–762. [[CrossRef](#)]
118. Iriarte, E.; Foyo, A.; Sánchez, M.A.; Tomillo, C.; Setién, J. The Origin and Geochemical Characterization of Red Ochres from the Tito Bustillo and Monte Castillo Caves (Northern Spain). *Archaeometry* **2009**, *2*, 231–251. [[CrossRef](#)]
119. Kingery-Schwartz, A.; Popelka-Filcoff, R.S.; Lopez, D.A.; Pottier, F.; Hill, P.; Glascock, M. Analysis of Geological Ochre: Its Geochemistry, Use, and Exchange in the US Northern Great Plains. *Open J. Archaeom.* **2013**, *1*, e15. [[CrossRef](#)]
120. Dimuccio, L.A.; Rodrigues, N.; Larocca, F.; Pratas, J.; Amado, A.M.; de Carvalho, L.A.E.B. Geochemical and Mineralogical Fingerprints to Distinguish the Exploited Ferruginous Mineralisations of Grotta Della Monaca (Calabria, Italy). *Spectrochim. Acta. A Mol. Biomol. Spectrosc.* **2017**, *173*, 704–720. [[CrossRef](#)]
121. Zipkin, A.M.; Ambrose, S.H.; Hanchar, J.M.; Piccoli, P.M.; Brooks, A.S.; Anthony, E.Y. Elemental Fingerprinting of Kenya Rift Valley Ochre Deposits for Provenance Studies of Rock Art and Archaeological Pigments. *Quat. Int.* **2017**, *430*, 42–59. [[CrossRef](#)]
122. Mauran, G.; Caron, B.; Dérozier, F.; Nankela, A.; Bahain, J.-J.; Pleurdeau, D.; Lebon, M. Data Pretreatment and Multivariate Analyses for Ochre Sourcing: Application to Leopard Cave (Erongo, Namibia). *J. Archaeol. Sci. Rep.* **2021**, *35*, 102757. [[CrossRef](#)]
123. Aitchison, J. The Statistical Analysis of Compositional Data. In *Monographs on Statistics and Applied Probability*; Chapman & Hall: London, UK, 1986; p. 416.
124. Comas-Cufí, M.; Thió-Henestrosa, S. CoDaPack 2.0: A Stand-Alone, Multi-Platform Compositional Software. In Proceedings of the CoDaWork'11: 4th International Workshop on Compositional Data Analysis, Girona, Spain, 9–13 May 2011.
125. How, M.W. *The Mountain Bushmen of Basutoland*; van Schaik, J.L., Ed.; Cambridge University Press: Cambridge, UK, 1962.
126. Pomiès, M.; Menu, M.; Vignaud, C. Tem Observations of Goethite Dehydration: Application to Archaeological Samples. *J. Eur. Ceram. Soc.* **1999**, *19*, 1605–1614. [[CrossRef](#)]

127. Lima de Faria, J. Dehydration of Goethite and Diaspore. *Z. Für Krist.* **1963**, *119*, 176–203. [[CrossRef](#)]
128. Watari, F.; van Landuyt, J.; Delavignette, P.; Amelinckx, S.; Igata, N. X-Ray Peak Broadening as a Result of Twin Formation in Some Oxides Derived by Dehydration. *Phys. Status Solidi A* **1982**, *73*, 215–224. [[CrossRef](#)]
129. Pomiès, M.-P.; Morin, G.; Vignaud, C. XRD Study of the Goethite-Hematite Transformation: Application to the Identification of Heated Prehistoric Pigments. *Eur. J. Solid State Inorg. Chem.* **1998**, *35*, 9–25. [[CrossRef](#)]
130. Gualteri, A.F.; Venturelli, P. In Situ Study of the Goethite-Hematite Phase Transformation by Real Time Synchrotron. *Am Miner.* **1999**, *84*, 895–904. [[CrossRef](#)]
131. Löffler, L.; Mäder, W. Anisotropic X-Ray Peak Broadening and Twin Formation in Hematite Derived from Natural and Synthetic Goethite. *J. Eur. Ceram. Soc.* **2006**, *26*, 131–139. [[CrossRef](#)]
132. De Faria, D.L.A.; Lopes, F.N. Heated Goethite and Natural Hematite: Can Raman Spectroscopy Be Used to Differentiate Them? *Vib. Spectrosc.* **2007**, *45*, 117–121. [[CrossRef](#)]
133. Zoppi, A.; Lofrumento, C.; Castellucci, E.M.; Sciau, P. Al-for-Fe Substitution in Hematite: The Effect of Low Al Concentrations in the Raman Spectrum of Fe<sub>2</sub>O<sub>3</sub>. *J. Raman Spectrosc.* **2008**, *39*, 40–46. [[CrossRef](#)]
134. Onoratini, G.; Perinet, G. Données Minéralogiques Sur Les Colorants Rouges Préhistoriques de Provence: Démonstration Que Certains d’entre Eux Ont Été Obtenus Par Calcination de Goethite. *Comptes Rendus Académie Sci.* **1985**, *301*, 119–124.
135. Baffier, D.; Girard, M.; Menu, M.; Vignaud, C. La Couleur à La Grande Grotte d’Arcysur-Cure (Yonne). *L’Anthropologie* **1999**, *1999*, 103–121.
136. Pomiès, M.-P.; Menu, M.; Vignaud, C.; Goupy, J.; Mohen, J.-P. Lascaux, pigments préhistoriques à base d’oxydes de fer: Hématite naturelle collectée ou goethite chauffée? In Proceedings of the Art et Chimie, la Couleur: Actes du Congrès, Paris, France, 16–18 September 1998.
137. Lahaye, C.; Godfrey-Smith, D.I.; Guibert, P.; Bechtel, F. Equivalent Thermal History (HE) of Ferruginous Sandstones Based on the Thermal Activation Characteristics of Quartz. *Radiat. Meas.* **2006**, *41*, 995–1000. [[CrossRef](#)]
138. Aitken, M.J. *Thermoluminescence Dating*; Academic Press: London, UK, 1985.
139. Dayet, L. Matériaux, Transformations et Fonctions de L’ocre Au Middle Stone Age: Le Cas de Diepkloof Rock Shelter Dans Le Contexte de L’Afrique Australe. Ph.D. Thesis, Université Bordeaux, Bordeaux, France, 2012.
140. Parkington, J.E.; Rigaud, J.-P.H.; Poggenpoel, C.; Porraz, G.; Texier, P.-J. Introduction to the Project and Excavation of Diepkloof Rock Shelter (Western Cape, South Africa): A View on the Middle Stone Age. *J. Archaeol. Sci.* **2013**, *40*, 3369–3375. [[CrossRef](#)]
141. Porraz, G.; Parkington, J.E.; Rigaud, J.-P.; Miller, C.E.; Poggenpoel, C.; Tribolo, C.; Archer, W.; Cartwright, C.R.; Charrié-Duhaut, A.; Dayet, L.; et al. The MSA Sequence of Diepkloof and the History of Southern African Late Pleistocene Populations. *J. Archaeol. Sci.* **2013**, *40*, 3542–3552. [[CrossRef](#)]
142. Tribolo, C.; Mercier, N.; Douville, E.; Joron, J.-L.; Reyss, J.-L.; Rufer, D.; Cantin, N.; Lefrais, Y.; Miller, C.E.; Porraz, G.; et al. OSL and TL Dating of the Middle Stone Age Sequence at Diepkloof Rock Shelter (South Africa): A Clarification. *J. Archaeol. Sci.* **2013**, *40*, 3401–3411. [[CrossRef](#)]
143. Calligaro, T.; MacArthur, J.D.; Salomon, J. An Improved Experimental Setup Analysis of Heavy and Light Elements Beam for the Simultaneous PIXE with a 3 MeV Proton External Beam. *Nucl. Instrum. Methods Phys. B* **1996**, *109–110*, 125–128. [[CrossRef](#)]
144. Swann, C.P.; Fleming, S.J. Selective Filtering in PIXE Spectrometry. *Nucl. Instrum. Methods Phys. Res. Sect. B Beam Interact. Mater. At.* **1990**, *49*, 65–69. [[CrossRef](#)]
145. Campbell, J.L.; Boyd, N.I.; Grassi, N.; Bonnicksen, P.; Maxwell, J.A. The Guelph PIXE Software Package IV. *Nucl. Instrum. Methods Phys. Res. Sect. B Beam Interact. Mater. At.* **2010**, *268*, 3356–3363. [[CrossRef](#)]
146. Miller, C.E.; Goldberg, P.; Berna, F. Geoarchaeological Investigations at Diepkloof Rock Shelter, Western Cape, South Africa. *J. Archaeol. Sci.* **2013**, *40*, 3432–3452. [[CrossRef](#)]
147. Schmidt, P.; Porraz, G.; Slodczyk, A.; Bellot-gurlet, L.; Archer, W.; Miller, C.E. Heat Treatment in the South African Middle Stone Age: Temperature Induced Transformations of Silcrete and Their Technological Implications. *J. Archaeol. Sci.* **2013**, *40*, 3519–3531. [[CrossRef](#)]
148. Porraz, G.; Texier, P.-J.; Archer, W.; Piboule, M.; Rigaud, J.-P.; Tribolo, C. Technological Successions in the Middle Stone Age Sequence of Diepkloof Rock Shelter, Western Cape, South Africa. *J. Archaeol. Sci.* **2013**, *40*, 3376–3400. [[CrossRef](#)]